JHEP

Published for SISSA by Springer

Received: May 12, 2014
Revised: September 2, 2014
Accepted: October 18, 2014
Published: November 12, 2014

Dark matter and dark force in the type-I inert 2HDM with local $\mathrm{U}(1)_H$ gauge symmetry

P. Ko,[a] **Yuji Omura**[b] **and Chaehyun Yu**[a]

[a] *School of Physics, KIAS, Seoul 130-722, Korea*
[b] *Department of Physics, Nagoya University, Nagoya 464-8602, Japan*

E-mail: pko@kias.re.kr, yujiomura3@gmail.com, chyu@kias.re.kr

Abstract: We discuss dark matter (DM) physics in the Type-I inert two-Higgs-doublet model (2HDM) with local $\mathrm{U}(1)_H$ Higgs gauge symmetry, which is assigned to the extra Higgs doublet in order to avoid the Higgs-mediated flavor problems. In this gauged inert DM setup, a $\mathrm{U}(1)_H$-charged scalar Φ is also introduced to break $\mathrm{U}(1)_H$ spontaneously through its nonzero vacuum expectation value (VEV), $\langle\Phi\rangle$, and then the remnant discrete subgroup appears according to the $\mathrm{U}(1)_H$ charge assignment of Φ. The $\mathrm{U}(1)_H$-charged Higgs doublet does not have Yukawa couplings with the Standard-Model (SM) fermions, and its lightest neutral scalar component H is stable because of the remnant discrete symmetry. In order to suppress a too large Z-exchange diagram contribution in DM direct detection experiments, we have to introduce a non-renormalizable operator which can be generated by integrating out an extra heavy scalar. With these new particles contents, we first investigate the constraint on the $\mathrm{U}(1)_H$ gauge interaction, especially through the kinetic and mass mixing between the SM gauge bosons and the extra gauge boson. Then we discuss dark matter physics in our 2HDM: thermal relic density, and direct/indirect detections of dark matter. The additional $\mathrm{U}(1)_H$ gauge interaction plays a crucial role in reducing the DM thermal relic density. The most important result within the inert DM model with local $\mathrm{U}(1)_H$ symmetry is that $\sim O(10)$ GeV dark matter scenario, which is strongly disfavored in the usual Inert Doublet Model (IDM) with Z_2 symmetry, is revived in our model because of newly open channels, $HH \to Z_H Z_H, Z_H Z$. Exotic Higgs decays, $h \to Z_H Z_H, Z Z_H$, would be distinctive signatures of the inert 2HDM with local $\mathrm{U}(1)_H$ symmetry.

Keywords: Higgs Physics, Beyond Standard Model, Cosmology of Theories beyond the SM

ArXiv ePrint: 1405.2138

doi:10.1007/JHEP11(2014)054

JHEP11(2014)054

Contents

JHEP11(2014)054

1 Introduction

The discovery of a Standard-Model-like Higgs boson at the LHC [1, 2] opens new era in particle physics and cosmology. The precise measurements of its mass and couplings to the Standard Model (SM) particles will reveal the structure of the Higgs sector, which is the least known piece in the SM. Up to now, its couplings to the ordinary particles are consistent with the predictions of the SM within uncertainties and most of results at the LHC can be understood in the framework of the SM [3, 4]. On the other hand, there are some clues on new physics beyond the SM: nonbaryonic dark matter (DM), dark energy, neutrino oscillation, baryon asymmetry of the universe, and etc., which cannot be explained by the renormalizable SM and require its extensions beyond the SM.

One simple extension of the SM is to add one extra Higgs doublet. In fact, many high-energy theories predict extra Higgs doublets, and the two-Higgs-doublet models (2HDMs)

could be interpreted as the effective theories of those high energy theories after we integrate out heavy particles. Of course, the 2HDMs could be interesting by themselves, because of their rich phenomenology and benchmark models with an extended Higgs sector. 2HDMs predict extra neutral and charged scalar bosons in addition to a SM-like Higgs boson, and the extra scalar bosons may change phenomenology of Higgs boson and SM particles at colliders [5]. We could also find cold dark matter candidates in some 2HDMs: one of the extra scalars [6–9] or one of the extra fermions, which may be added to the models in 2HDMs with gauged $U(1)_H$ symmetry [10]. When the Higgs potential in 2HDMs has a CP-violating source, the baryon asymmetry of the universe may be explained [11]. And small neutrino masses may naturally be generated by one-loop diagram in some 2HDMs [12]. Finally, it is very interesting that in 2HDMs with flavor-dependent $U(1)_H$ gauge symmetry, the anomalies in the top forward-backward asymmetry at the Tevatron and $B \to D^{(*)}\tau\nu$ decays at BABAR may be reconciled [13–18].

One important phenomenological issue in models with extra Higgs doublets is the so-called Higgs-mediated flavor changing neutral current (FCNC) problem. If a right-handed (RH) fermion couples with more than two Higgs doublets, FCNCs involving the neutral scalar bosons generally appear after the electro-weak (EW) symmetry breaking. In many cases, this Higgs-mediated flavor problem is resolved by imposing softly-broken Z_2 symmetry á la Glashow and Weinberg [19]. The discrete Z_2 symmetry could be replaced by other discrete symmetry [20] or continuous local gauge symmetry [10]. In fact, the present authors proposed a new class of 2HDMs where $U(1)_H$ Higgs gauge symmetry is introduced instead of softly broken discrete Z_2 symmetry, in order to avoid the flavor problem [10], and discussed the phenomenology of Type-I 2HDM with $U(1)_H$ in ref. [21]. When Higgs doublets are charged under the extra gauge symmetry, the so-called ρ parameter is deviated from the SM prediction at the tree level if the $U(1)_H$-charged Higgs doublet develops a nonzero vacuum expectation value (VEV). In ref. [21], the authors investigate the constraints not only from the EW precision observables (EWPOs) but also from the recent LHC results on the SM-like Higgs search, especially in Type-I 2HDMs where only one Higgs doublet is charged and the SM particles are neutral under $U(1)_H$. The deviation of the ρ parameter is mainly from the tree-level mass mixing between Z and the $U(1)_H$ gauge boson (Z_H), and from the mass differences among the scalar bosons. The bounds on EWPOs require small $U(1)_H$ interactions, so that its effects become tiny in physical observables.

In this work, we consider a new scenario where the VEV of the $U(1)_H$-charged Higgs doublet is zero in our Type-I 2HDM and a $U(1)_H$-charged SM-singlet scalar Φ breaks $U(1)_H$ spontaneously. In this case, the mass mixing between gauge bosons is also negligible at the tree level. Therefore we can expect that the Z_H gauge interaction becomes sizable and then the idea of gauged $U(1)_H$ Higgs symmetry might be tested. The bounds on Z_H mass and its couplings to the SM particles will come from the loop-level mass and kinetic mixings between the SM gauge bosons and Z_H, as well as the tree-level kinetic mixing.

On the other hand, the SM fermions are chiral under new $U(1)_H$ gauge symmetry, so that the model may be anomalous unless new chiral fermions are introduced. As discussed in refs. [10, 21], we could consider the anomaly-free $U(1)_H$ charge assignment to build the

JHEP11(2014)054

2HDM with local Higgs symmetry: for example, the SM particles are not charged and only one extra Higgs doublet is charged under $U(1)_H$. In our 2HDM, the $U(1)_H$ will be broken by the nonzero VEV of Φ. However, the residual symmetry may still remain and we could find stable cold dark matter (CDM) candidates. In section 3, we introduce the conditions for the stability of DM candidates and discuss dark matter physics in the Type-I 2HDMs with local $U(1)_H$ gauge symmetry. One well-known dark matter model among 2HDMs is the so-called inert doublet model (IDM) [6–9, 22]. In the ordinary IDM, one extra Z_2 symmetry is imposed and the extra Higgs doublet is the only Z_2-odd particle. If the Higgs doublet does not develop the nonzero VEV, Z_2 symmetry forbids the decay of the lightest Z_2-odd scalar boson, and the scalar boson could be a good CDM candidate. The scalar CDM interacts with the SM particle through the scalar exchange and the EW interaction, and one could find the favored regions for the correct thermal relic density around $m_{\rm DM} \sim 60\,{\rm GeV}$ or $m_{\rm DM} > 500\,{\rm GeV}$ [6–9], which are safe for the constraints from the collider searches and the DM direct detection searches. Especially, the light CDM scenario faces the strong bound from the invisible search at the LHC, and the only allowed mass region is around the resonance of the SM-Higgs.

In our 2HDM with local $U(1)_H$ gauge symmetry, at least one Higgs doublet is charged under the $U(1)_H$ symmetry, and the scalar component respects the remnant discrete symmetry of $U(1)_H$ after the EW and $U(1)_H$ symmetry breaking. This discrete symmetry originates from the local $U(1)_H$ and will protect the DM from decay to all orders in perturbation theory even in the presence of higher dimensional operators. Stability of the scalar DM is guaranteed by the local discrete symmetry, and the scalar DM interacts with the SM particles strongly through the $U(1)_H$ gauge interaction. The extension of the usual IDM to the $U(1)_H$ gauge symmetric one not only suggests the origin of the Z_2 Higgs symmetry, but also may open up a new scenario for dark matter phenomenology, which cannot be achieved in the usual IDM. In fact, the $U(1)_H$ gauge interaction can plays an important role in thermalizing the scalar DM, and $\sim O(10)\,{\rm GeV}$ CDM scenario could be revived in our IDM, which is a very interesting aspect of our model. In section 4.1 and section 4.2, we investigate the constraints on not only the relic density and the DM direct detection, but also the DM indirect detection, in the IDM with Z_2 symmetry (IDMwZ_2) and in the IDM with local $U(1)_H$ symmetry (IDMwU$(1)_H$). The indirect astrophysical observations would be one of the ways to prove our model so that we calculate the velocity-averaged cross section for dark matter annihilation in the halo, and consider the constraints from the Fermi-LAT by observing the γ-ray flux from the dwarf spheroidal galaxies, which is one of the recent results relevant to the light CDM scenario.

The organization of this paper is as follows. In section 2, we introduce the Lagrangian of the Type-I 2HDM with $U(1)_H$ Higgs symmetry and discuss the constraints on the $U(1)_H$ gauge interactions. In section 3, we discuss dark matter physics in the IDMwZ_2 and IDMwU$(1)_H$: the stability of CDM, the thermal relic density, the DM direct and indirect detections. Section 5 is devoted to our conclusion.

JHEP11(2014)054

2 2HDM with $U(1)_H$ Higgs symmetry

Based on ref. [21], we discuss our setup of the Type-I 2HDM with $U(1)_H$ Higgs symmetry, where only extra Higgs doublet H_1 is charged under the $U(1)_H$ gauge symmetry and all the SM particles including the SM Higgs doublet H_2 are neutral. The Lagrangian for gauge fields and scalar fields is given by

$$\begin{aligned}\mathcal{L} = &-\frac{1}{4}F_Y^{\mu\nu}F_{Y\mu\nu} - \frac{1}{4}F^{a\mu\nu}_{\mathrm{SU(2)_L}}F^{a}_{\mathrm{SU(2)_L}\mu\nu} - \frac{1}{4}F_H^{\mu\nu}F_{H\mu\nu} - \frac{\kappa}{2}F_Y^{\mu\nu}F_{H\mu\nu} \\ &+\left|\left(\partial_\mu - \frac{i}{2}g'B_\mu - \frac{i}{2}gA^a_\mu\tau^a - iq_{H_1}g_H\hat{Z}_{H\mu}\right)H_1\right|^2 \\ &+\left|\left(\partial_\mu - \frac{i}{2}g'B_\mu - \frac{i}{2}gA^a_\mu\tau^a\right)H_2\right|^2 + \left|(\partial_\mu - iq_\Phi g_H\hat{Z}_{H\mu})\Phi\right|^2 - V_{\mathrm{scalar}}(H_1,H_2,\Phi), \end{aligned} \tag{2.1}$$

where $F_Y^{\mu\nu}$, $F^{a\mu\nu}_{\mathrm{SU(2)_L}}$, and $F_H^{\mu\nu}$ are the field strengths of $U(1)_Y$, $SU(2)_L$, and $U(1)_H$ of the gauge fields, B^μ, A^a_μ, and $\hat{Z}^\mu_H$, and g', g and g_H are their gauge couplings. q_{H_1} is the $U(1)_H$ charge of H_1. κ is the kinetic mixing between $U(1)_Y$ and $U(1)_H$ field strength tensors, which is allowed by the local gauge symmetry. It is assumed to be a free parameter. Finally $V_{\mathrm{scalar}}(H)$ is the potential for the complex scalars:

$$\begin{aligned}V_{\mathrm{scalar}} = &(m_1^2 + \widetilde{\lambda}_1|\Phi|^2)H_1^\dagger H_1 + (m_2^2 + \widetilde{\lambda}_2|\Phi|^2)H_2^\dagger H_2 \\ &+\frac{\lambda_1}{2}(H_1^\dagger H_1)^2 + \frac{\lambda_2}{2}(H_2^\dagger H_2)^2 + \lambda_3(H_1^\dagger H_1)(H_2^\dagger H_2) + \lambda_4|H_1^\dagger H_2|^2 \\ &+m_\Phi^2|\Phi|^2 + \lambda_\Phi|\Phi|^4 + c_l\left(\frac{\Phi}{\Lambda_\Phi}\right)^l(H_1^\dagger H_2)^2 + h.c.. \end{aligned} \tag{2.2}$$

A new scalar Φ is a singlet under the SM gauge group, but is charged under $U(1)_H$ gauge symmetry, and thus it breaks the $U(1)_H$ by the nonzero VEV ($\langle\Phi\rangle \equiv v_\Phi$). c_l is the dimensionless coupling of the higher-dimension operator, which is suppressed by one arbitrary scale (Λ_Φ), to make the mass difference between a CP-even scalar and a pseudoscalar bosons. Note that only $(H_1^\dagger H_2)^2$ term can be multiplied by $U(1)_H$-charged operator $(\Phi/\Lambda_\Phi)^l$, whereas $(\Phi^\dagger\Phi/\Lambda_\Phi^2)^n$ term can be multiplied to all terms because of $U(1)_H$ gauge invariance. If both are included, we would lose predictability because of too many non-renormalizable interactions. Therefore we will choose $U(1)_H$ charge judiciously and $l = 1$ is allowed by $U(1)_H$ gauge symmetry. Then the leading nonrenormalizable operator would be dim-5 operator (the $c_{l=1}$ term), and other operators with $(\Phi^\dagger\Phi/\Lambda^2)^n$ would be at least dim-6 or higher. The single unique dim-5 operator would lift up the mass degeneracy between a CP-even scalar and a pseudoscalar bosons by spontaneous $U(1)_H$ breaking. Therefore we do not lose predictability much even if we consider nonrenormalizable operators. We also give comment on how to realize c_l in section 3. $(H_1^\dagger H_2)$ term may be also allowed, multiplying $(\Phi/\Lambda_\Phi)^l$ following the $U(1)_H$ charge assignment. This term may cause the nonzero VEV of H_1, so that we define the charge assignment to forbid this term, as we see in section 3.

After the EW and $U(1)_H$ symmetry breaking, the VEVs of H_i and Φ give the masses of the gauge bosons. In general, the kinetic mixing between the SM gauge bosons and $\hat{Z}_H$

JHEP11(2014)054

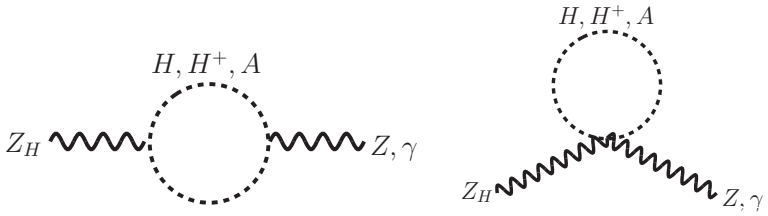

Figure 1. The one-loop contribution of the extra scalars to Z_H-Z and Z_H-γ mixing in the IDMwU(1)$_H$ model.

may be generated as follows,

$$\begin{aligned}\mathcal{L}_{\text{eff}} = &-\frac{1}{4}F_Z^{\mu\nu}F_{Z\mu\nu} - \frac{1}{4}F_\gamma^{\mu\nu}F_{\gamma\mu\nu} - \frac{1}{4}F_H^{\mu\nu}F_{H\mu\nu} - \frac{\kappa_Z}{2}F_Z^{\mu\nu}F_{H\mu\nu} - \frac{\kappa_\gamma}{2}F_\gamma^{\mu\nu}F_{H\mu\nu} \\ &+\frac{1}{2}\hat{M}_Z^2\hat{Z}^\mu\hat{Z}_\mu + \frac{1}{2}\hat{M}_{Z_H}^2\hat{Z}_H^\mu\hat{Z}_{H\mu} + \Delta M_{Z_HZ}^2\hat{Z}^\mu\hat{Z}_{H\mu}. \end{aligned} \tag{2.3}$$

If $\langle H_1\rangle$ is nonzero, $\Delta M_{Z_HZ}^2$ will be generated at the tree level. When $\langle H_1\rangle$ is zero, the tree-level mixing of Z and Z_H does not exist, but the mixing may occur at the loop level, as shown in the next subsection.

2.1 Mass mixing and kinetic mixing at the one-loop level

Before the EW and U(1)$_H$ gauge symmetry breaking, the local gauge symmetry forbids the mass mixing and the kinetic mixing among neutral gauge bosons, except for the kinetic mixing κ term in eq. (2.1). If we assume that κ is negligible, $\hat{Z}_H$ does not couple with the SM fermions.

After the EW and U(1)$_H$ symmetry breaking, the mass mixing and the extra kinetic mixings, κ_Z and κ_γ, will appear at the loop level, even if κ is negligible at the EW scale. The one-loop contributions of the extra scalars to κ_Z and κ_γ are, for instance, given in figure 1. For nonzero $\langle H_1\rangle$, they are evaluated as

$$\kappa_Z = \frac{q_H g_H e c_W}{16\pi^2 s_W}\left\{\cos^2\beta Z_{WW} + \sin^2\beta Z_{H^+H^+} - c_{\chi_1}^{A_l}c_{H_1}^{h_m}(c_{\chi_1}^{A_l}c_{H_1}^{h_m} + c_{\chi_2}^{A_l}c_{H_2}^{h_m})Z_{A_lh_m}\right\}, \tag{2.4}$$

$$\kappa_\gamma = \frac{q_H g_H e}{16\pi^2}\left\{\cos^2\beta Z_{WW} + \sin^2\beta Z_{H^+H^+} - c_{\chi_1}^{A_l}c_{H_1}^{h_m}(c_{\chi_1}^{A_l}c_{H_1}^{h_m} + c_{\chi_2}^{A_l}c_{H_2}^{h_m})Z_{A_lh_m}\right\}, \tag{2.5}$$

where Z_{ab} is defined as

$$Z_{ab} = \frac{1}{3}\ln\left(\frac{\Lambda^2}{m_a^2}\right) + \frac{1}{6}\frac{m_a^2 - m_b^2}{m_a^2}. \tag{2.6}$$

Λ is the cut-off scale, but $\kappa_{Z,\gamma}$ are independent of Λ because the Λ dependence is canceled in $\kappa_{Z,\gamma}$. $c_{H_i}^{h_m}$ and $c_{\chi_i}^{A_m}$ are mixing angles of the CP-even and CP-odd scalars, which are defined by

$$H_i^0 = c_{H_i}^{h_m}h_m,\ \ \chi_i = c_{\chi_i}^{A_m}A_m, \tag{2.7}$$

where $\{h_m, A_l\}(\{H_i^0, \chi_i\})$ are the CP-even and CP-odd scalars in the mass (interaction) bases, respectively, and the formulas for $\{h_m, A_l\}(\{H_i^0, \chi_i\})$ are referred to ref. [21]. In the ordinary 2HDM, $\tan\beta$ is defined as $\tan\beta = \langle H_2^0\rangle/\langle H_1^0\rangle$, and $\langle H_1\rangle = 0$ corresponds to

JHEP11(2014)054

$\cos\beta = 0$. In this limit, the physical neutral scalars can be expressed as $h = h_2\cos\alpha - h_\Phi \sin\alpha$, $H = h_1$, and $\tilde{h} = h_2\sin\alpha + h_\Phi\cos\alpha$, where h_1, h_2, and h_Φ are the CP-even neutral components of H_1, H_2, and Φ after symmetry breaking, respectively, and α is the mixing angle between h_2 and h_Φ, where $\Phi = (v_\Phi + h_\Phi + i\chi_\Phi)/\sqrt{2}$ and $H_2^0 = (v + h_2 + i\chi_2)/\sqrt{2}$. The mass mixing, $\Delta M^2_{Z_H Z}$, is also induced at the one-loop level through the diagrams in figure 1,

$$\Delta M^2_{Z_H Z} = -\frac{q_H g_H e}{16\pi^2 s_W c_W} F(m^2_{A_l}, m^2_{h_m})\{c^{A_l}_{\chi_1} c^{h_m}_{H_1}(c^{A_l}_{\chi_1} c^{h_m}_{H_1} + c^{A_l}_{\chi_2} c^{h_m}_{H_2})\}. \tag{2.8}$$

In the limit $\cos\beta \to 0$, which corresponds to $\langle H_1^0\rangle \to 0$, the mixing parameters converge to

$$\kappa_Z = \frac{q_H g_H e c_W}{16\pi^2 s_W}\left\{\frac{1}{3}\ln\left(\frac{m_A^2}{m_{H^+}^2}\right) - \frac{1}{6}\frac{m_A^2 - m_H^2}{m_A^2}\right\}, \tag{2.9}$$

$$\kappa_\gamma = \frac{q_H g_H e}{16\pi^2}\left\{\frac{1}{3}\ln\left(\frac{m_A^2}{m_{H^+}^2}\right) - \frac{1}{6}\frac{m_A^2 - m_H^2}{m_A^2}\right\}, \tag{2.10}$$

$$\Delta M^2_{Z_H Z} = -\frac{q_H g_H e}{32\pi^2 s_W c_W}(m_A^2 - m_H^2). \tag{2.11}$$

Thus the mass and kinetic mixings of the gauge bosons are generated radiatively, even if the tree-level mass mixing is negligible.

The $\mathrm{U}(1)_H$ gauge coupling g_H will be constrained by the collider experimental results through the couplings of Z_H with the SM fermions induced by the radiative corrections. Even if κ is zero at the cut-off scale (Λ), it may become sizable at the low scale through the RG running. In fact, the RG running correction can easily enhance the mixing in the case with large g_H. For example, the RG flow of κ_γ is estimated as

$$\kappa_\gamma(\mu) \approx \kappa_\gamma(\Lambda) + \frac{q_H}{48\pi^2} g_H e \ln\left(\frac{\mu^2}{\Lambda^2}\right), \tag{2.12}$$

assuming that the running corrections of e and g_H are small. Eventually, g_H could be large if the masses of scalars are degenerate, but such large g_H coupling would enhance the kinetic mixing easily. In our analyses, we set the cut-off scalar (Λ) at 1 TeV, and include the radiative corrections to κ, assuming $\kappa(\Lambda) = 0$.

2.2 Constraints on Z_H coupling from the mixings

The kinetic mixings and the mass mixing could be interpreted as the coupling of Z_H, after changing the interaction basis to the mass basis. Assuming that the mixing angles are small enough, the couplings could be described as

$$g_Z Z_\mu J_Z^\mu + e A_\mu J_\gamma^\mu + \{g_Z(\xi - \kappa_Z) J_Z^\mu - 2e\kappa_\gamma J_\gamma^\mu\} Z_{H\mu}, \tag{2.13}$$

where a mixing angle ξ is given by the mass mixing,

$$\tan 2\xi = \frac{2\Delta M^2_{Z_H Z}}{\hat{M}^2_{Z_H} - \hat{M}^2_Z}. \tag{2.14}$$

JHEP11(2014)054

The mixings among neutral gauge bosons are strongly constrained by the EWPOs and Z' searches at high energy colliders, as discussed in ref. [21]. If Z_H is heavier than the center-of-mass energy of LEP (209 GeV), we can derive the bound on the effective coupling of Z_H [23–25], depending on the Z_H mass. The lower bound on M_{Z_H}/g_H would be $\sim O(10)$ TeV [24, 25]. If Z_H is lighter than 209 GeV, the upper bound of Z_H coupling would be $O(10^{-2})$ in order that we avoid conflicts with the data from $e^+e^- \to f^-f^+$ ($f = e, \mu$) [24–26]. If Z_H is lighter than M_Z, the upper bound on the kinetic mixing is $\kappa \lesssim 0.03$ [27, 28]. In the very light Z_H region (100 MeV $\lesssim M_{Z_H} \lesssim$ 10 GeV), the strong bound comes from the BaBar experiment, $\kappa \lesssim O(10^{-3})$ [28].

The upper bounds on the Z_H production at the Tevatron and LHC are investigated in the processes, $pp(\overline{p}) \to Z_H X \to f\overline{f}X$ [23, 26, 29, 30], and the stringent bound requires $O(10^{-3})$ times smaller couplings than the Z-boson couplings around $M_{Z_H} = 300$ GeV [30].

If we require the conservative bound $\sin\xi \lesssim 10^{-3}$, according to ref. [30], we could estimate the upper bound in the large $\tan\beta$ case as follows, based on the eqs. (2.9), (2.10), and (2.11),

$$q_{H_1} g_H \left| \ln\left(\frac{m_A^2}{m_{H^+}^2}\right)\right| \lesssim 0.28, \;\; q_{H_1} g_H \left|\frac{m_A^2 - m_H^2}{\hat{M}_{Z_H}^2 - \hat{M}_Z^2}\right| \lesssim 0.43. \tag{2.15}$$

Including the bounds from the scalar searches, we see the allowed region for g_H and M_{Z_H} in figure 2 in the case with $\langle H_1^0\rangle = 0$ ($\cos\beta = 0$).

2.3 Constraints on the scalar bosons in the 2HDM with $\cos\beta = 0$

In the limit $\cos\beta \to 0$, the new U(1)$_H$ gauge interaction could be large because the constraint from the ρ parameter is drastically relaxed. At the tree level, the ρ parameter constraint in general two Higgs doublet model with U(1)$_H$ symmetry (2HDMwU(1)$_H$) is given by [10]

$$\{q_{H_1}(\cos\beta)^2 + q_{H_2}(\sin\beta)^2\}^2 \frac{g_H^2}{g_Z^2}\frac{M_{\hat{Z}}^2}{M_{\hat{Z}_H}^2 - M_{\hat{Z}}^2} \lesssim O(10^{-3}), \tag{2.16}$$

with $M_{\hat{Z}}^2 = g_Z^2 v^2$ and $M_{\hat{Z}_H}^2 = g_H^2 v^2 (q_{H_1}^2 \cos^2\beta + q_{H_2}^2 \sin^2\beta) + g_H^2 q_\Phi^2 v_\Phi^2$, where $q_{H_1,H_2,\Phi}$'s are the U(1)$_H$ charges of H_1, H_2 and Φ, respectively.

Now in the Type-I 2HDMs the SM Higgs doublet and all the SM fields are U(1)$_H$ neutral so that $q_{H_2} = 0$. In the IDM which we take into account for analysis in this paper, $\langle H_1\rangle = 0$, namely $\cos\beta = 0$. Then eq. (2.16) implies that the $\Delta\rho$ constraint disappears at the tree level, and the U(1)$_H$ gauge coupling g_H can be large. Also Z_H gets its mass only from the VEV of the Φ field and can be relatively light. Furthermore, the scalar component of H_1 may be stable and could be a good cold dark matter candidate, as we discuss in the next section. Below, we introduce the constraints on the extra scalars from the collider experiments and EWPOs.

2.3.1 Constraints on the extra scalar bosons

When H_1 does not develop a nonzero VEV, the scalar components in H_1, (H, A, H^+), are in the mass eigenstate and do not have the Yukawa couplings with the SM fermions. This corresponds to the setup of the IDM [6–9, 22]. If H is the lightest particle, A and H^+ decay to

JHEP11(2014)054

H and on-shell or off-shell Z, Z_H, W^+. The constraints on H, A, and H^+ from the collider experiments have been widely discussed in the framework of the IDM [31–35]. The search for multi leptons plus missing energy at LEP gives the lower bounds: $m_{H^+} \gtrsim 90\,\text{GeV}$ and $m_A \gtrsim 100\,\text{GeV}$ with $m_A - m_H \gtrsim 8\,\text{GeV}$. The exotic Z decay may be kinematically forbidden by the condition, $m_A + m_H > M_Z$ in order not to change the decay width of the Z boson.

The mass differences between m_{H^+} and $m_A(m_H)$ are also strongly constrained by the EWPOs, and it has been studied in the Type-I 2HDMwU(1)$_H$ in the case with large scalar masses and generic $\tan\beta$ [21]. When $\tan\beta$ is large, the mass difference between the heavy CP-even scalar boson (H) and the massive CP-odd scalar boson (A) becomes small and the phase of Φ is eaten by $\hat{Z}_H$. $\tan\beta = 0$ makes the masses degenerate in our 2HDM with $c_l = 0$ in eq. (2.2), even after the EW and U(1)$_H$ symmetry breaking. When H and A are degenerate and become CDM candidates, the Z boson exchange diagram enhances the DM direct detection cross section, for example, through $H + N \to A + N$, where N is a nucleon, and the CDM scenario would be excluded immediately by the XENON100 and LUX experiments. A small mass difference ($\gtrsim O(100)$ keV) between H and A would be enough to suppress the direct detection cross section. In the 2HDMs with Z_2 symmetry, such a term is generated by λ_5 term,

$$\mathcal{L}_{\lambda_5} = \frac{\lambda_5}{2}(H_1^\dagger H_2)^2 + H.c. \tag{2.17}$$

which is clearly invariant under the usual discrete Z_2 symmetry, $(H_1, H_2) \to (-H_1, +H_2)$. However this terms is not allowed if we implement the discrete Z_2 symmetry to continuous U(1)$_H$ gauge symmetry at the renormalizable level. Still the effective λ_5 term may be induced by higher-dimensional operators integrating out heavy particles as we discuss below (see below, section 3.2).

2.3.2 Constraints from exotic SM-like Higgs decays

The IDM condition $\cos\beta = 0$ realizes the situation that H_1 completely decouples with the SM fermions, so that the scalar components could be very light because of the relaxed experimental bounds, and the SM-like Higgs may decay to the extra scalar bosons, as well as Z_H and Φ,

$$h \to HH, AA, H^+H^-, \widetilde{h}\widetilde{h}, ZZ_H, Z_HZ_H,$$

where $\widetilde{h}$ is the CP-even scalar mainly from Φ. Including H^+ loop corrections, $h \to Z_H\gamma$ will open. The extra scalars affect the signal strength μ of the SM-like Higgs boson at the LHC, where μ is defined in ref. [21]. As discussed in refs. [36–38], $\mu_{\gamma\gamma}$ could be enhanced if H^+ is light. However, it is difficult to enhance μ_{ZZ} in the Type-I 2HDM. When the extra fermions should be introduced to cancel the gauge anomaly, which may appear according to the U(1)$_H$ charge assignments to the SM fermions, μ_{ZZ} could be enhanced from the contribution of color-charged extra fermions to the $gg \to h$ production. Now the ATLAS experiment shows a small enhancement for $\mu_{\gamma\gamma}^{ggF+t\bar{t}h}$ and $\mu_{ZZ}^{ggF+t\bar{t}h}$ [39, 40], but the CMS results for $\mu_{\gamma\gamma}^{ggF+t\bar{t}h}$ and $\mu_{ZZ}^{ggF+t\bar{t}h}$ are consistent with the SM prediction within 1σ error [41, 42]. In this paper, we assume the SM-like Higgs boson and adopt the

JHEP11(2014)054

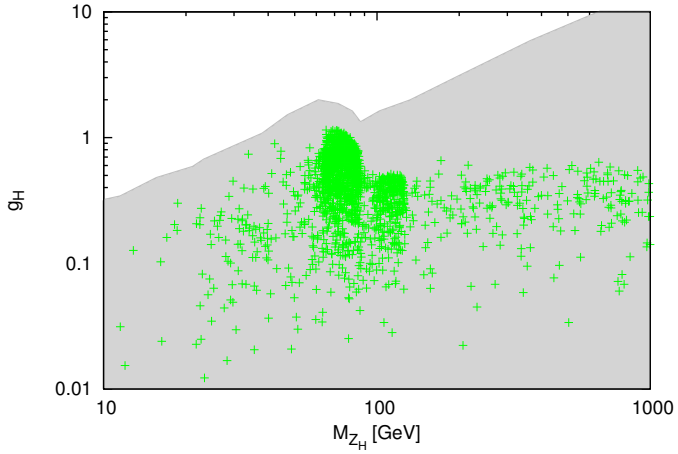

Figure 2. Allowed region in the (M_{Z_H}, g_H) plane with $\cos\beta = 0$ in the IDMwU(1)$_H$. We have imposed the bounds from the collider search as well as EWPOs. The gray region satisfy the bounds from the thermal relic density for the CDM at Planck and the dark matter direct detection search at LUX. The green points are also allowed by the dark matter indirect detection search at Fermi-LAT.

CMS results for simplicity. Specifically, we impose the constraints on the signal strengths: $\mu^{gg}_{\gamma\gamma} = 0.70^{+0.33}_{-0.29}$ and $\mu^{gg}_{ZZ} = 0.86^{+0.32}_{-0.26}$ [41–43].

When the Z_H boson is light, the SM-like Higgs boson h may decay into $Z_H Z_H$ or $Z Z_H$. If the mass of the dark matter H is less than the half of the SM-like Higgs mass (m_h), h also can decay invisibly into HH. These exotic h decays are strongly constrained by the search for the invisible and/or nonstandard Higgs decays at the LHC [44, 45]. We set the bound on the exotic Higgs decay to be [46–48]

$$\frac{\sigma^{Vh}_{\rm 2HDM}}{\sigma^{Vh}_{\rm SM}} \times [{\rm BR}(h \to Z Z_H) \text{ or } {\rm BR}(h \to Z_H Z_H)] \leq 0.69, \tag{2.18}$$

where $\sigma^{Vh}_{\rm SM,2HDM}$ is the cross section for the Vh production in the SM and in the 2HDM, respectively, and ${\rm BR}(h \to Z_{(H)} Z_H)$ is the branching ratio for the $h \to Z_{(H)} Z_H$ decay.

In figure 2, the allowed region for M_{Z_H} and g_H is shown in gray color by taking into account the constraints from the Z-Z_H mixing, EWPOs, search for exotic scalars, vacuum stability and unitarity, based on the above arguments and ref. [21]. For the numerical calculation we choose the following parameter spaces: 20 GeV $\leq m_H, M_{Z_H} \leq$ 1000 GeV, 90 GeV $\leq m_{H^+} \leq$ 200 GeV, 63 GeV $\leq m_{\tilde{h}} \leq$ 200 GeV, $0 \leq \alpha \leq 2\pi$, $0 \leq g_H \leq 4\pi$, $0 \leq \lambda_1 \leq 4\pi$, $0 \leq |\lambda_3|, |\tilde{\lambda}_1| \leq 4\pi$, and $-0.2 \leq \lambda_5 \leq 0$. λ_4 is derived as $\lambda_4 = 2(m^2_H - m^2_{H^+})/v - \lambda_5$.

Since the SM fermions do not have the U(1)$_H$ charge, the relatively large g_H is allowed as shown in eq. (2.15). In the small M_{Z_H} region, g_H is $\sim O(0.1)$, but it can be $O(1)$ just below the Z pole and much higher in the large M_{Z_H} region. We note that the gray region in figure 2 also satisfies the constraints from the thermal relic density of the CDM, DM direct detection searches at the CDMSII, XENON100 and LUX experiments, while the green points satisfy the DM indirect detection search at Fermi-LAT as well as the relic

JHEP11(2014)054

density and the DM direct detection search, which we will discuss in the following section. In the small M_{Z_H} region, the allowed values of g_H do not change significantly even if we include the constraints from the DM indirect detection search. However, in the large M_{Z_H} region, g_H should be less than $O(1)$ when the constraints from the DM indirect detection search are taken into account. This is because one of the main channels for the annihilation of dark matters in this region is $HH \to ZZ_H$, which would gives a stronger bound on g_H.

3 How to stabilize dark matter in the IDMwU(1)$_H$

In this section, we introduce a dark matter candidate in the IDMwU(1)$_H$ and compare predictions in the IDMwU(1)$_H$ with those in the IDMwZ_2 [6–9]. As we discussed in section 2, there is a U(1)$_H$ gauge boson as well as a U(1)$_H$-charged Higgs doublet in our Type-I 2HDM with U(1)$_H$. If the Higgs doublet H_1 does not develop a VEV, one of the scalar components of the doublet is a CDM candidate and the correct thermal relic density could be achieved. First of all, let us discuss the stability of the dark matter in a generic U(1)$_H$ symmetric model in the section 3.1, and then discuss dark matter physics in the IDMwU(1)$_H$.

3.1 General conditions for DM stability

In general, we could build a gauge extension of the SM, such as U(1)$_H$. As discussed in ref. [10], not only additional Higgs doublets but also extra fermions may have to be introduced in order to satisfy the anomaly-free conditions, depending on the charge assignment. The gauge symmetry would be spontaneously broken by extra scalars to avoid an extra massless gauge boson. Still, we could expect that there could be a residual local discrete symmetry after the spontaneous gauge symmetry breaking. Then, if the extra fermions and/or scalars may respect the residual symmetry, their decays may be forbidden by the remaining local discrete symmetry.

Let us discuss the generic U(1)$_H$ symmetric models with matters ψ_I and Φ whose charges are q_I and q_Φ. ψ_I are U(1)$_H$-charged extra fields. Simply, let us assume that U(1)$_H$ is broken only by a nonzero VEV of Φ. Generally, the charges can be described as

$$\{q_\Phi, q_I\} = \left\{\frac{n_\Phi}{N}, \frac{n_I}{N}\right\}, \tag{3.1}$$

where n_I, n_Φ and N are integers, and all the charges are irreducible fractions. Now, we consider the case $\langle\Phi\rangle \neq 0$. In order to have a residual discrete symmetry after U(1)$_H$ breaking, the Φ field should be a singlet under the residual one after the U(1)$_H$ symmetry breaking. When we assume that U(1)$_H$ breaks down to Z_m symmetry, the integers (m, m') can be defined by the relation,

$$\exp\left(i\frac{2\pi m'}{m}\frac{n_\Phi}{N}\right)\Phi = \Phi. \tag{3.2}$$

This could be satisfied by $(m, m') = (n_\Phi, N)$ and we find that the residual symmetry is

$$\text{U}(1)_H \to Z_{|n_\Phi|}. \tag{3.3}$$

JHEP11(2014)054

In our 2HDM with $U(1)_H$, two fields H_1 and Φ are charged under $U(1)_H$. If H_1 also develops a nonzero VEV, $\langle H_1 \rangle$ may also break the $Z_{|n_\Phi|}$. It depends on q_{H_1}, and the charge assignment may be fixed by the $H_1^\dagger H_2$ term, namely by the operator

$$\mu_n \Phi^n H_1^\dagger H_2. \tag{3.4}$$

This term should be forbidden because it will correspond to the tadpole term of H_1 which causes nonzero $\langle H_1 \rangle$ when H_2 and Φ break the EW and $U(1)_H$ symmetries by their nonzero VEVs. Furthermore, if the μ_n term is allowed, the relation of the charges, $n_{H_1} = n n_\Phi$, is required, so that H_1 is singlet under $Z_{|n_\Phi|}$, as far as n is an integer. In the next section, we discuss the IDMw$U(1)_H$ where only Φ breaks $U(1)_H$. q_{H_1} is defined as $q_{H_1}/q_\Phi = n_{H_1}/n_\Phi$ is not an integer to realize a stable particle.

3.2 Toward the IDMw$U(1)_H$

One of the motivations for considering Type-I 2HDMs could be CDM, which can be realized in the so-called inert 2HDM (IDMwZ_2), where one of the extra neutral scalar bosons could be a good CDM candidate.

In the usual IDMwZ_2, all the SM particles including the SM Higgs doublet with nonzero VEV are Z_2-even, whereas the other Higgs doublet without nonzero VEV is Z_2-odd.[1] Then the scalar component of the Z_2-odd doublet could be stable and could be a good CDM candidate, if the Higgs doublet does not get a nonzero VEV. One of the main issue in this type of CDM models is to generate mass differences among the charged, CP-odd, and CP-even components of the Z_2-odd doublet, in order to avoid strong constraints from the collider experiments and the direct dark matter searches. In the IDMwZ_2, the $\lambda_4 |H_1^\dagger H_2|^2$ and $\lambda_5 (H_1^\dagger H_2)^2$ terms in the Higgs potential play an important role in the mass spectrum. Especially the λ_5 term shifts the pseudoscalar mass and thereby suppresses kinematically the interaction of the CP-even component with a nucleus (N) through the Z exchange.

In the IDMw$U(1)_H$, the discrete Z_2 symmetry is gauged to continuous local $U(1)_H$ symmetry, so that massless $U(1)_H$ gauge boson is predicted if the stability of dark matter is guaranteed by $U(1)_H$ Higgs gauge symmetry. The $U(1)_H$ symmetry could be spontaneously broken, introducing SM singlet scalar Φ with a nonzero $U(1)_H$ charge q_Φ. According to the general discussion in the previous subsection, the scalar components of H_1 could be stable if $\langle H_1 \rangle = 0$ and q_{H_1}/q_Φ is not an integer. However, the $U(1)_H$ symmetric Higgs potential generates an extra flat direction, so that H and A tend to be degenerate. In fact, the $U(1)_H$ symmetry forbids the λ_5 term at the tree level, which was the origin of the mass difference in the ordinary IDMwZ_2. Without the λ_5 term, too large cross section for the direct detection of dark matter will be predicted, which is in serious conflict with the data. In order to avoid this catastrophe,we generate the effective λ_5 term from higher-dimensional operators, such as the c_l term in eq. (2.2). Then the λ_5 term depends on $\langle \Phi \rangle$ in this scenario.

One simple way to realize higher-dimensional operators for an effective λ_5 term is to introduce an extra complex scalar (φ) with a nonzero $U(1)_H$ charge and $\langle \phi \rangle = 0$. Let us

[1] Here Z_2 symmetry is presumed to be a global symmetry.

JHEP11(2014)054

consider the following renormalizable potential among the scalar bosons:

$$V_\Phi(|\Phi|^2, |\varphi|^2) + V_H(H_i, H_i^\dagger) + \lambda_\varphi(\Phi)\varphi^2 + \lambda_H(\varphi)H_1^\dagger H_2 + h.c.. \tag{3.5}$$

where λ_H and λ_φ are functions of φ and Φ, respectively, and respect the local $U(1)_H$ gauge symmetry as well as the SM gauge symmetries. Only Φ breaks $U(1)_H$ and only H_2 breaks the EW symmetry, due to nonzero values of V_Φ and V_H. Now we assume that φ does not develop a nonzero VEV, and the direct coupling between H_i and Φ is forbidden by a suitable choice of q_Φ. If $U(1)_H$ is spontaneously broken by the nonzero $\langle\Phi\rangle$, the squared mass difference (Δm^2) between real and imaginary components of φ will be generated by the λ_φ term. Assuming that φ is heavier than the EW scale and $\lambda_H = \lambda_H^0\varphi$, λ_5 is induced effectively at low energy when we integrate out the φ field:

$$\lambda_5 \sim \frac{(\lambda_H^0)^2}{2}\frac{\Delta m^2}{m_{\varphi_R}^2 m_{\varphi_I}^2}, \tag{3.6}$$

where m_{φ_R} and m_{φ_I} are the masses of the real and imaginary parts of the complex scalar φ. After the $U(1)_H$ symmetry breaking, the effective scalar potential is the same as the one of the IDMwZ_2, so that the small mass difference between H and A can be achieved, and we can evade the strong bound from the direct detection search for dark matter.

4 DM phenomenology in IDMwU(1)$_H$

Base on the above argument and the setup, we discuss the dark matter physics in IDMwU(1)$_H$ and compare the results of the IDMwU(1)$_H$ with the ones of the IDMwZ_2.

4.1 Relic density and direct detection

The most recent measurement for the DM relic density carried out by the PLANCK Collaboration yields its value to be [49]

$$\Omega_{\rm CDM}h^2 = 0.1199 \pm 0.0027. \tag{4.1}$$

We impose that thermal relic densities calculated in the IDMwZ_2 and IDMwU(1)$_H$ satisfy this bound within 3σ deviation, assuming that the scalar dark matter in the IDMwZ_2 or IDMwU(1)$_H$ is the only CDM of the universe. In case we assume that there exist another dark matter particles which contribute to the dark matter relic density, we impose the bound $\Omega_{\rm IDM} \leq 0.1280$.

On the other hand, dark matter may interact with atomic nuclei in a detector, and it can be detected by underground experiments, such as the DAMA [50], CoGeNT [51], CRESST [52], XENON [53, 54], CDMS [55], LUX [56] and etc. The CoGeNT, DAMA, CRESST-II, and CDMS-II experiments show some excesses in the light dark matter region with the dark matter mass of about 10 GeV and the spin-independent cross section for the WIMP-nucleon scattering is predicted to be $\sigma_{\rm SI} \sim 10^{-40} - 10^{-42}$ cm^2 [55]. It is interesting that the four experiments have some excesses in the similar dark matter mass region, but the measured spin-independent cross section is different by about two orders of magnitude

JHEP11(2014)054

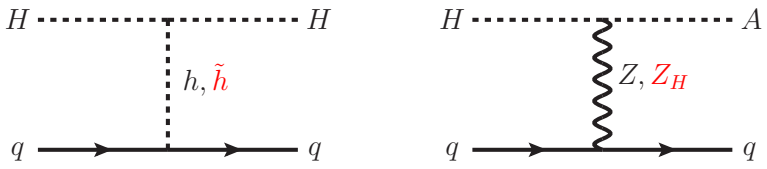

Figure 3. Feynman diagrams for direct detection of DM in the usual IDMwZ_2 and additional ones in the gauged U(1)$_H$ model, IDMwU(1)$_H$. Note that $\tilde{h}$ and Z_H do not exist in the usual IDMwZ_2.

from each other. Also these signals are almost ruled out by the XENON100 and LUX experiments, where the upper bound for the spin-independent cross section is $\sim 10^{-45}$ cm^2 at $m_H \sim 33\,\mathrm{GeV}$ and and $\sim 10^{-44}$ cm^2 at $m_H \sim 10\,\mathrm{GeV}$ [53, 54, 56]. The positive signals might be accommodated with each other while being reconciled with the XENON100 and LUX results by introducing isospin-violating dark matter [57] or exothermic inelastic DM scattering.

In our model, we assume that the positive signals at low DM mass regions are excluded by the XENON100 and LUX experiments and impose the bound for the spin-independent scattering cross section for the dark matter and nucleon from the LUX experiment. In figure 3, we draw Feynman diagrams which dominantly contribute to the direct detection of dark matter. When the mass difference is negligible between m_H and m_A, the Z and Z_H exchange diagrams become dominant and the spin-independent cross section for the dark matter candidate and nucleon could exceed the bounds from the LUX experiment. This problem is easily cured by the generation of the mass difference between m_H and m_A with a sizable λ_5 term. Then we can ignore Z and Z_H exchanges in figure 3, and the scalar $(h, \tilde{h})$ exchange is dominant in the direct cross section:

$$\sigma_{SI} = \frac{\mu^2 f^2 m_N^2}{4\pi m_H^2} \left\{ \left(\frac{\cos^2\alpha}{m_h^2} + \frac{\sin^2\alpha}{m_{\tilde{h}}^2} \right) (\lambda_3 + \lambda_4 + \lambda_5) + \left(\frac{1}{m_h^2} - \frac{1}{m_{\tilde{h}}^2} \right) \frac{v_\Phi \widetilde{\lambda}_1 \cos\alpha \sin\alpha}{v} \right\}^2 , \tag{4.2}$$

where f is the form factor, μ is the reduced mass of the DM-nucleon system, m_N is the mass of the nucleon and α is the mixing angle between h_Φ and H_2^0. We calculate the elastic cross section of the scattering of H on atomic nuclei by using micrOMEGAs, where the velocity of H near the Earth, $v_H \approx 0.001c$ [58]. In figure 5, we show our predictions in this model. All the points in figure 5 pass the bound from the LUX experiment, as well as the collider experiments, which we described in section 2.

Thermal relic density, direct detections and indirect detection of DM in the IDMwZ_2 have been studied extensively in the literature (see, for example, [6–9, 59–69]). In the IDMwZ_2, the extra scalars annihilate into two fermions through the SM-Higgs exchanging and two gauge bosons, as we see in figure 4. There are two interesting scenarios: light dark matter ($m_H \lesssim M_Z$) and heavy dark matter ($m_H \gtrsim 500\mathrm{GeV}$). In figure 5, we show the relic densities (a) in the light H scenario and (b) in the heavy H scenario, respectively. The pink points correspond to the IDMwZ_2, whereas the cyan points to the IDMwU(1)$_H$. The horizontal line is the current value of the DM thermal relic density.

JHEP11(2014)054

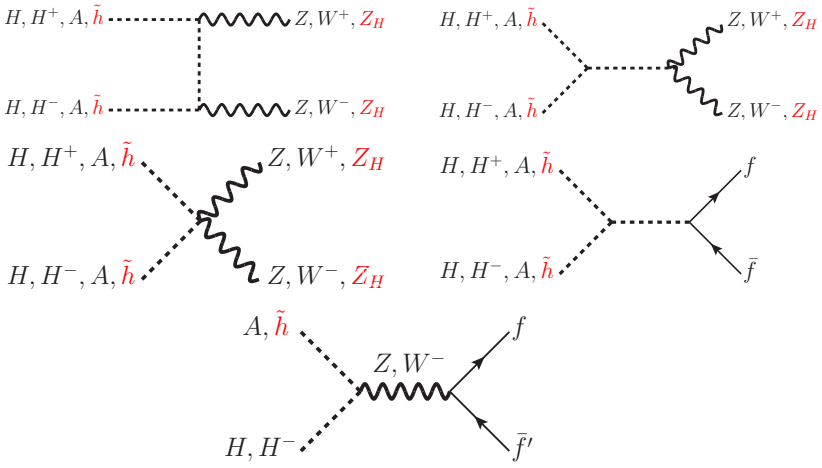

Figure 4. Feynman diagrams for (Co)annihilation of dark matters in IDMwZ_2 and IDMwU(1). The red ones are from Φ and Z_H in the gauged U(1)$_H$ model, IDMwU(1). Dotted, solid and wavy lines denote spin-0, 1/2 and spin-1 particles, respectively.

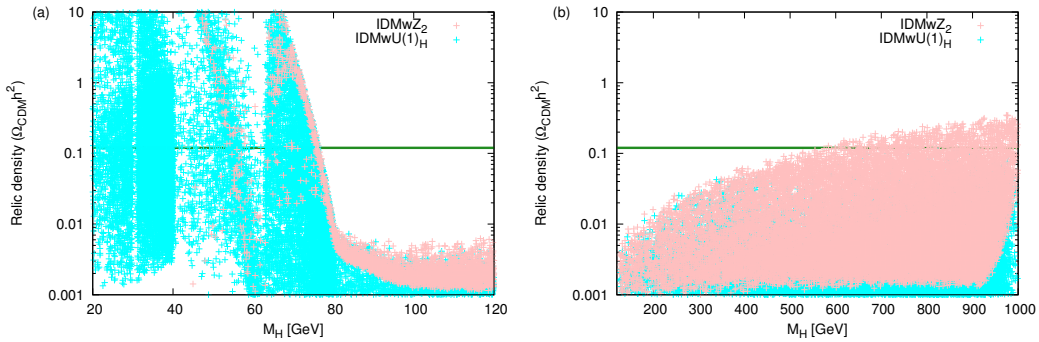

Figure 5. M_H and Ωh^2 (a) in the light H scenario and (b) in the heavy H scenario.

4.1.1 The case of IDM with Z_2 symmetry

Let us first explain the results of the IDMwZ_2. In the light dark matter scenario, the dark matter pair annihilation into the SM fermions ($HH \to f\bar{f}$) through the s-channel exchange of the SM Higgs boson h makes a dominant contribution to the relic density in the range of $m_H \lesssim 50\,\text{GeV}$. However the direct detection experiments of DM [53, 56] and the invisible decay of the SM-like Higgs boson [46–48] strongly constrain the $h - H - H$ coupling. Therefore the annihilation in that light mass region cannot be large enough to thermalize the scalar DM, and the light CDM scenario has been already excluded, as we see in figure 5.

In the h resonance region, $m_H \sim m_h/2 \sim 60\,\text{GeV}$, the annihilation cross section is enhanced and the thermal relic density could be below the current observation. In the region with $m_H \gtrsim m_W$, the annihilation channels, $HH \to WW$ and $HH \to ZZ$ are open so that the IDMwZ_2 predicts the small relic density in figure 5. The co-annihilation of H and $A(H^+)$ also becomes relevant in the region with $40\,\text{GeV} \lesssim m_H \lesssim 80\,\text{GeV}$, if the mass difference between H and $A(H^+)$ is small. In this case, the pair annihilation of H^+H^- or

JHEP11(2014)054

AA could also be relevant in the region $m_H \gtrsim 80\,\mathrm{GeV}$, and their contribution to the relic density could reach 60% of the relic density in a certain parameter region.

In the heavy dark matter scenario, $HH \to ZZ, W^+W^-$ processes are very efficient and many channels like $HH \to hh, t\bar{t}$ are open. They can easily reduce the DM thermal relic density. As shown in figure 5 (b), the relic density is below the current data in the region $m_H \lesssim 500\,\mathrm{GeV}$, and we have to consider extra DM species in order to account for the DM relic density in eq. (4.1). If we wish to accommodate the current data on the DM relic density within uncertainties in the IDMwZ_2, the DM mass m_H should be greater than 500 GeV in the heavy dark matter scenario. The pair annihilations of H^+H^- and AA also contribute to the DM relic density in the region where the mass difference between H^+, A and H is small, but the ratio of their contribution to the relic density is less than 0.5. Typically the $HH \to W^+W^-$ process makes a dominant contribution to the DM relic density. But in some parameter spaces the contribution of the pair annihilation of H^+H^- and AA to the relic density can be higher than that of the pair annihilation of HH. The process $HH \to hh$ can be relevant in some parameter spaces, but the ratio of the contribution is less than 0.3.

4.1.2 The case of IDM with local U(1)$_H$ symmetry

Now let us discuss the result in the IDMwU(1)$_H$, the main theme of this paper. In the IDMwU(1)$_H$, the new processes involving Z_H could be dominant in the annihilation of the CDM. For example, if Z_H is lighter than H, the $HH \to Z_H Z_H$ process is open and the Z_H decays to the SM fermions through the $Z - Z_H$ mixing. We can see the relevant annihilation modes in figure 3. Φ may also work as the mediator if it is light. Figure 5 (a) shows the relic density in the case $m_H \lesssim 126\,\mathrm{GeV}$. We also assume that M_{Z_H} is also smaller than 126 GeV because the result in the limit $m_{Z_H} \gg m_H$ would not be different from that in the IDMwZ_2. If $M_Z + M_{Z_H} < 2m_H$, then the $HH \to ZZ_H$ channel is also open and it gives another contribution to the CDM relic density. The new channels involving Z_H('s) could be dominant because of the weak bound on g_H in figure 2, and we could find the annihilations to Z_H and SM gauge bosons play a role in decreasing the relic density in figure 5 (a). Especially, we can find many allowed points in the region with $m_H \lesssim 40\,\mathrm{GeV}$ in the IDMwU(1)$_H$ (cyan points in figure 5 (a)), unlike the IDMwZ_2 case where the relic density becomes too large for $m_H \lesssim 40\,\mathrm{GeV}$. In this region, the gauge coupling g_H of U(1)$_H$ prefers a small value, $g_H \lesssim 0.5$ as shown in figure 2.

In the heavy H scenario, the qualitative feature in the IDMwU(1)$_H$ is similar to that in the IDMwZ_2 as shown in figure 5 (b). For $m_H \lesssim 500\,\mathrm{GeV}$, the predicted DM relic density is below the current value and another dark matter is required to make up for the deficit. In the region $m_H \gtrsim 500\,\mathrm{GeV}$, we can find the parameter regions which satisfy the current relic density. In most parameter spaces, the predicted DM density in the IDMwU(1)$_H$ is slightly smaller than that in the IDMwZ_2. This is because the new channels like $HH \to Z_H Z_H$ and $HH \to ZZ_H$ are open in the heavy CDM case, too, so that they yield an extra contribution to the dark matter density.

JHEP11(2014)054

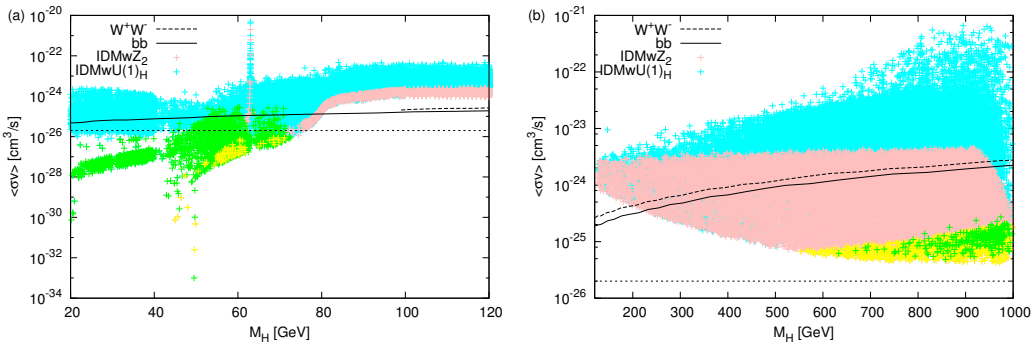

Figure 6. M_H in unit of GeV and $\langle\sigma v\rangle$ in unit of cm^3/s (a) in the light H scenario and (b) in the heavy H scenario. The pink and cyan points satisfy the constraints from the relic density and LUX experiments in the IDMwZ_2 and in the IDMwU$(1)_H$, respectively. The yellow and green points additionally satisfy the indirect constraints, $\Phi_{\rm PP} \leq 9.3 \times 10^{-30}\mathrm{cm}^3\mathrm{s}^{-1}\mathrm{GeV}^{-2}$ in the IDMwZ_2 and in the IDMwU$(1)_H$, respectively.

4.2 Constraints from indirect detection

In the IDMwU$(1)_H$, the light Z_H gauge boson may open the new annihilation channels of the CDM: $HH \to Z_H Z_H, ZZ_H, \gamma Z_H$. The Z_H contributions could be dominant in the relic density because of the large g_H, and then astrophysical observations may give a crucial bound on the Z_H-dominant scenario, as we discuss below. In the heavy H scenario, the HH annihilation to the SM particles could be dominant because of gauge interactions. In figure 4, we depict representative Feynman diagrams contributing to the HH annihilation.

In the galactic halo, the DM pair annihilation may occur and can be observed through the products of the annihilation: γ-rays, positrons, antiprotons, and etc.[2] This means that the detection of large signals for the γ-rays, positrons or antiprotons over astrophysical backgrounds would indicate indirect evidence for the dark matter annihilation. There are some tantalizing excesses in the mono-energetic gamma ray signal around 135 GeV observed by the Fermi-LAT [70–75] and in the positron excesses at a few GeV $\sim$ TeV scale observed by PAMELA, Fermi, and AMS02 Collaborations [76–78]. However, it is still unclear that the origin of the excesses comes from annihilation or decay of dark matter or astrophysical backgrounds [79, 80]. In this paper, we assume that the excesses are originated in the astrophysical phenomena. Then, indirect detection of dark matter plays a role in constraining models.

Many experiments are devoted to measure the products of the dark matter annihilation typically by observing cosmic rays from dwarf spheroidal satellite galaxies [81–84] and galactic center [85]. Especially, the dwarf spheroidal satellite galaxies of the Milky Way are excellent targets for the detection of the dark matter annihilation because of its large dark matter content and low astrophysical backgrounds like a hot gas. We calculate the

[2]If DM is not absolutely stable but lives much longer than the age of the universe, DM decays would produce similar observable effects in cosmic rays. In this paper we consider the case that DM is absolutely stable due to the remnant discrete symmetry of U$(1)_H$ gauge symmetry.

JHEP11(2014)054

velocity-averaged cross section for the dark matter annihilation in the dwarf spheroidal galaxies by using micrOMEGAs [58].

The integrated γ-ray flux ϕ, is divided two parts

$$\phi_s(\Delta\Omega) = \Phi_{\rm PP} \times J, \tag{4.3}$$

where the second part is related to the dark matter distribution in the galactic halo. Under the Navarro-Frenk-White density profile of dark matter [86] the J factor of each dwarf galaxy is given in refs. [87–90]. The quantity $\Phi_{\rm PP}$ for the self-conjugate particles is defined by

$$\Phi_{\rm PP} = \frac{\langle\sigma v\rangle}{8\pi m_H^2} \int_{E_{\rm min}}^{E_{\rm max}} \sum_f B_f \frac{dN_\gamma^f}{dE_\gamma} dE_\gamma, \tag{4.4}$$

where $\langle\sigma v\rangle$ is the velocity-averaged annihilation cross section, B_f is the branching ratio for each channel $XX \to ff'$, where f and f' could be the SM particle or new particle, and dN_γ^f/dE_γ is the photon energy spectrum for each annihilation channel. We note that the direct γ-ray production from the dark matter annihilation which yields the mono-energetic signal is loop-suppressed in both the IDMwZ_2 and the IDMwU(1)$_H$. The photon energy spectrum depends on the decay patterns of intermediate states f and f'.

4.2.1 The case of the IDM with Z_2 symmetry

First, we consider the velocity-averaged annihilation cross section in the IDMwZ_2 by using micrOMEGAs. Figure 6 shows $\langle\sigma v\rangle$ in units of cm^3/s (a) in the light H scenario and (b) in the heavy H scenario. The pink and yellow points correspond to the IDMwZ_2 while the cyan and green points to the IDMwU(1)$_H$, respectively. All the points satisfy thermal relic density and the direct detection constraint from the LUX experiments. And yellow and green points satisfy the additional constraints from indirect detections. The horizontal line around 3×10^{-26}cm^3/s is the bound from the relic density when the s-wave annihilation of dark matters is dominant. The upper region of this line would be allowed for the s-wave annihilation dominant case. The solid and dotted curves are the bounds from the Fermi-LAT experiment by assuming that the dominant annihilation channel is $HH \to b\bar{b}$ and $HH \to W^+W^-$. The lower region of these curves is allowed if the dominant annihilation channel is $HH \to b\bar{b}$ or $HH \to W^+W^-$. We note that all the points in figure 6 satisfy the constraints from the LUX experiment and their relic densities are below the current bound.

In the light H scenario, the $HH \to b\bar{b}$ process can be dominant in the Higgs-resonant region ($m_H \simeq 60\,$GeV), whereas the $HH \to WW$ process becomes dominant both in the Higgs-resonant region and in the region $m_H \simeq 80\,$GeV. In these regions, the bounds from the Fermi-LAT experiment might constrain directly the IDMwU(1)$_H$ as well as the IDMwZ_2. From figure 6 (a), we can find the allowed parameter spaces in the Higgs-resonant region, but there is no allowed point at $m_H \gtrsim 80\,$GeV. We note that the region for $m_H \lesssim 40\,$GeV is not allowed in the IDMwZ_2 because of overclosing of the Universe. As we will see in the next subsection, this conclusion changes completely when we extend the discrete Z_2 symmetry to local U(1)$_H$ symmetry because new channels open, namely $HH \to Z_H Z_H, Z_H Z$ for on-shell or off-shell Z.

JHEP11(2014)054

In the heavy H scenario, the contribution of the $HH \to b\bar{b}$ process is negligible and the $HH \to W^+W^-, ZZ$ processes become effective in the IDMwZ_2. Depending on the coupling to the SM-like Higgs boson, the $HH \to hh$ process could become dominant over the $HH \to W^+W^-$ process. In the $HH \to W^+W^-$ dominant case, we can use the bounds from the Fermi-LAT experiment. We note that in the IDMwZ_2, $\langle \sigma v \rangle$ is less than about 3×10^{-24} cm^3/s. In the region $m_H \gtrsim 200\,\mathrm{GeV}$, there might be the parameter region allowed from the γ-ray observation by the Fermi-LAT when the dominant DM annihilation channel is $HH \to W^+W^-$.

4.2.2 The case of IDM with local U(1)$_H$ symmetry

In figure 6, the cyan and green points depict the velocity-averaged annihilation cross section $\langle \sigma v \rangle$ versus the dark matter mass m_H in the IDMwU(1)$_H$. We note that all points satisfy the bounds from the direct detection search of dark matter at the LUX and the upper bound of the relic density, and the green points satisfy additional constraints from the indirect detection.

In the light H scenario (figure 6a), the allowed region in the IDMwU(1)$_H$ is much broader than that in the IDMwZ_2 because of additional channels like $HH \to Z_H Z_H$ and $HH \to ZZ_H$. In the region $m_H \gtrsim 80\,\mathrm{GeV}$, the overall feature is the same as in the IDMwZ_2 except that in the IDMwU(1)$_H$, $\langle \sigma v \rangle$ could be larger by an order of magnitude because of newly open channels such as $HH \to Z_H Z_H, Z_H Z$, etc. In the Higgs-resonant region, $m_H \sim 60\,\mathrm{GeV}$, we find that some points are allowed from the indirect detection search at the Fermi-LAT if the dominant annihilation process is $HH \to b\bar{b}$. As we already discussed in the previous subsection, there are no allowed points below $m_H \simeq 40\,\mathrm{GeV}$ in the IDMwZ_2, because the model predicts too large relic density. However, in the $O(10)$GeV CDM scenario of the IDMwU(1)$_H$, we can find the allowed parameter spaces which satisfy the constraints from the relic density and the direct detection search of dark matter. In this region, the dominant annihilation channels are $HH \to Z_H Z_H$ and $HH \to ZZ_H$, so that we cannot apply the constraints from the indirect detection search of dark matter directly.

In the heavy H scenario, the allowed parameter region from direct detection search for dark matter and relic density in the IDMwU(1)$_H$ is broader than in the IDMwZ_2. In this scenario, typically the $HH \to W^+W^-, ZZ$ or $HH \to hh$ processes could be dominant like the IDMwZ_2. However, in the IDMwU(1)$_H$, the $HH \to Z_H Z_H$ or $HH \to ZZ_H$ could be dominant processes over the $HH \to W^+W^-, ZZ, hh$ processes, depending on the values of the parameters in the model. It turns out that the $HH \to Z_H Z_H$ process could become dominant at $m_H \gtrsim 500\,\mathrm{GeV}$, whereas the $HH \to ZZ_H$ process could dominate over the other processes at $m_H \gtrsim 200\,\mathrm{GeV}$.

4.2.3 Φ_{PP}

In the case that the $HH \to Z_H Z_H$ and $HH \to ZZ_H$ processes are dominant over other processes in the IDMwU(1)$_H$, we cannot apply the bound from the indirect detection search of dark matter at the Fermi-LAT, which assumes that annihilation into the $b\bar{b}$ or W^+W^- pair is dominant. The γ-ray spectrum strongly depends on the decay pattern of particles produced from the dark matter annihilation. The Z_H boson dominantly decays into a pair

JHEP11(2014)054

	m_H	m_{H^+}	$m_{\tilde{h}}$	M_{Z_H}	m_A	g_H	λ_5	λ_1	λ_3	$\tilde{\lambda}_1$	α	Ωh^2	$\langle\sigma v\rangle_0$
L1	38.6	189	91.6	39.2	110	0.33	−0.174	2.38	1.09	−2.37	0.035	0.113	0.086
L2	53.8	194	73.2	29.6	108	0.215	−0.144	5.79	1.09	−1.59	0.047	0.117	2.20
H1	821	822	661	985	827	0.235	−0.164	3.87	0.15	−0.429	6.24	0.119	5.89

Table 1. Benchmark points in the IDMwU(1)$_H$. All the masses m_H, m_{H^+}, $m_{\tilde{h}}$, M_{Z_H} and m_A are in unit of GeV, the mixing angle α is in radian, and $\langle\sigma v\rangle_0$ is in unit of 10^{-26} cm^3/s, respectively.

of SM fermions through the Z-Z_H mixing and its decay pattern is similar to that of the SM Z boson. In this case, the main source of the γ-ray would be the $HH \to Z_H Z_H(Z) \to b\bar{b}b\bar{b}$ process. The γ-ray spectrum produced from this process would be different from the one from $HH \to b\bar{b}$. Therefore we should not apply the bound from the Fermi-LAT shown in figure 6 directly.

In order to find out if our models can satisfy the constraints from the indirect detection search at the Fermi-LAT, we compute the quantity $\Phi_{\rm PP}$ in eq. (4.4) by using micrOMEGAs. The range of the photon energy from 500 MeV to 500 GeV is summed. For the comparison, we use the value in ref. [82], which was obtained by using the joint analysis of seven Milky Way dwarfs and Pass 7 data from the Fermi Gamma-ray Space Telescope. A 95% upper bound is $\Phi_{\rm PP} = 5.0^{+4.3}_{-4.5} \times 10^{-30}{\rm cm}^3{\rm s}^{-1}{\rm GeV}^{-2}$ [82]. In figure 6, the green points satisfy this upper limit in the IDMwU(1)$_H$ while the yellow points satisfy this limit in the IDMwZ_2. The pink and cyan points predict more γ-ray than the upper limit.

In the light H scenario, only the Higgs-resonant region is allowed in the IDMwZ_2, but the region $m_H \lesssim 40\,{\rm GeV}$ is allowed in the IDMwU(1)$_H$ too. In the Higgs-resonant region, $\langle\sigma v\rangle$ in some parameter spaces is below the reference line for the s-wave annihilation dominant case at the decoupling temperature of dark matter. There are two sources for the smaller $\langle\sigma v\rangle$ in the present universe. At the decoupling temperature, the velocity of dark matter is $O(0.1)$, but the velocity at the halo is $O(0.001)$. Another source is that the co-annihilation of HH^+ or HA and pair annihilation of AA or H^+H^- also contribute to the relic density, but the co-annihilation does not appear in the halo at the current temperature. In the region $m_H \lesssim 40\,{\rm GeV}$, only IDMwU(1)$_H$ can have a proper dark matter model to explain the bounds from the relic density, the direct and indirect detection searches of dark matter. In this region, most of points predict smaller $\langle\sigma v\rangle$ than the reference line for the s-wave dominant annihilation case. We find that the $HH \to Z_{(H)} Z_H$ process is dominant in this case and $m_{Z_H} \approx m_H$. In this quasi-degenerate case, there is a suppression factor in the phase space, which is proportional to the velocity of dark matter. This can explain the gap of about $O(0.01 \sim 0.001)$ in $\langle\sigma v\rangle$.

In the heavy H scenario, the allowed region appear at $m_H \gtrsim 500\,{\rm GeV}$ in both the IDMwZ_2 and IDMwU(1)$_H$. Most of points predict smaller relic density than the observed one at the Planck experiment, but some of them predict the exact relic density within 3σ uncertainties. We note that the spin-averaged annihilation cross section in the halo at the zero temperature is over the reference line in the whole region. We find that the contribution of HH annihilation to the relic density is at most 90% of the total relic density predicted in the

JHEP11(2014)054

model. Remaining the relic density is accounted for by the co-annihilation of HH^+ or HA and/or the pair annihilation of AA or H^+H^-, which do not occur in the present halo. This may explain the small gap between the reference line and the predicted $\langle\sigma v\rangle$ in the models.

4.3 Three benchmark points for illustration

Since our model has many parameters, we choose three benchmark points for which we can discuss the underlying physics in a more transparent manner. In table 1, we show three benchmark points, all of which are safe for the astrophysical observations discussed above: the 1st one in the light dark matter region ($L1$), the 2nd one in the h resonance region ($L2$), and the 3rd one in the heavy dark matter region ($H1$).

At the $L1$ point, the dark matter mass is $m_H = 38.6\,\mathrm{GeV}$, while the $\mathrm{U}(1)_H$ gauge boson mass is $M_{Z_H} = 39.2\,\mathrm{GeV}$, which is almost the same as m_H. The coupling $\lambda_5 = -0.174$ generates the mass difference between A and H with $m_A = 110\,\mathrm{GeV}$, where the $HN \to AN$ process through the Z or Z_H exchange is kinematically forbidden and we can evade the strong bound from the direct detection search of dark matter. $\lambda_4 = -0.957$ and the spin-independent cross section for the WIMP-nucleon scattering is $\sigma_{\mathrm{SI}} = 2.3 \times 10^{-46}\ \mathrm{cm}^2$, which is below the LUX bound at $m_H \sim 38\,\mathrm{GeV}$. The corresponding relic density of DM is $\Omega h^2 = 0.113$, where $HH \to Z_H Z_H$ is the dominant channel for the correct thermal relic density. The DM annihilation cross section at the present universe is $\langle\sigma v\rangle_0 = 8.6 \times 10^{-28}$ cm^3/s, where the $HH \to ZZ_H$ process contributes to the annihilation of HH by 98% and the $HH \to b\bar{b}$ process is about 2%.

At the $L2$ point, $m_H = 53.8\,\mathrm{GeV}$ and $M_{Z_H} = 29.6\,\mathrm{GeV}$. $\lambda_5 = -0.144$, which leads to $m_A = 108\,\mathrm{GeV}$. The mass difference between H and A is large enough to avoid the LUX bound and the spin-independent cross section for the H and nucleon is $\sigma_{\mathrm{SI}} = 2.9 \times 10^{-46}$ cm^2, which is below the LUX bound. Here, $\lambda_4 = -0.999$. The relic density is $\Omega h^2 = 0.117$, where the contribution of $HH \to Z_H Z_H$ to the relic density is 52% and that of $HH \to b\bar{b}$ is 34%. Finally the DM annihilation cross section at the present universe is $\langle\sigma v\rangle_0 = 2.20 \times 10^{-26}$ cm^3/s. The contribution of $HH \to ZZ_H$ to $\langle\sigma v\rangle_0$ is 52% and that of $HH \to Z_H Z_H$ is 45%.

At the $H1$ point, $m_H = 821\,\mathrm{GeV}$ and $M_{Z_H} = 985\,\mathrm{GeV}$. $\lambda_5 = -0.164$, which leads to $m_A = 827\,\mathrm{GeV}$. In this case, H^+ and A are almost degenerate to H, but still $m_A - m_H = 6\,\mathrm{GeV}$, which is large enough that one can evade the strong bound from the direct detection experiments. $\lambda_4 = 0.086$ and the spin-independent cross section for the H and nucleon is $\sigma_{\mathrm{SI}} = 6.1 \times 10^{-46}\ \mathrm{cm}^2$, which is below the LUX bound. The relic density is $\Omega h^2 = 0.119$ and a lot of processes contribute to the relic density because dark matter is much heavier than the SM particles ($m_H \gg m_W, m_Z, m_f$). The contribution of each process of $HH \to ZZ_H, W^+W^-$, $H^+H^- \to W^+W^-, AZ_H$ is 11%, 10%, 9%, and 9%, respectively. Besides these processes, many processes for HH, H^+H^+, H^+H^-, H^+H annihilation and so on contribute to the relic density. The DM annihilation cross section at the present universe is $\langle\sigma v\rangle_0 = 5.89 \times 10^{-26}$ cm^3/s. The contributions of $HH \to ZZ_H$, $HH \to W^+W^-$, and $HH \to ZZ$ to $\langle\sigma v\rangle$ are 34%, 31%, and 23%, respectively. Those of $HH \to hh, AW^+W^-, t\bar{t}$ are less than 8%.

JHEP11(2014)054

In summary, three benchmark points have qualitatively different mass spectra and couplings. Still we find that all these three points produce acceptable phenomenology for the Higgs boson(s) and DM. The inert 2HDM with local $U(1)_H$ gauge symmetry has rich phenomenology due to new particles introduced by local $U(1)_H$ gauge symmetry. In particular, light DM ($\lesssim 60\,\text{GeV}$) is still allowed in the gauged inert 2HDM (IDMw$U(1)_H$), unlike the usual inert 2HDM (IDMwZ_2) where DM below $\sim 60\,\text{GeV}$ is excluded, because of the strong bound from the direct detection cross section, thermal relic condition and the invisible decay of the SM Higgs. New particles and new interactions in the gauge $U(1)_H$ model help to cure these problems in the IDMwZ_2, when suitable particle spectra and proper couplings are chosen in the IDMw$U(1)_H$.

5 Conclusion

In this paper, we constructed inert 2HDM with local $U(1)_H$ gauge symmetry instead of the usual discrete Z_2 symmetry. In this IDMw$U(1)_H$, the $U(1)_H$ gauge symmetry is spontaneously broken by a nonzero VEV of a $U(1)_H$-charged SM-singlet scalar Φ. The $U(1)_H$-charged new Higgs doublet H_1 neither couples to the SM fermions nor develops a nonzero VEV. The new Higgs doublet H_1 can be decomposed into a CP-even, CP-odd, and charged scalars ($H, A, H^\pm$, respectively), and one of the neutral scalar bosons (either H or A) could be a good CDM candidate because of the discrete Z_2 Higgs gauge symmetry, which is a remnant of the original $U(1)_H$ gauge symmetry spontaneously broken by nonzero $\langle\Phi\rangle$. At the renormalizable level with these particle contents, H and A are degenerate in mass, and the model is immediately excluded by the strong constraints from direct detection experiments on the Z exchange to $HN \to AN$. This problem can be solved by lifting the mass degeneracy between the DM H and the pseudoscalar A by introducing another $U(1)_H$-charged SM-singlet scalar φ which does not develop nonzero VEV. This new singlet scalar φ induces an effective λ_5 coupling as described in eq. (24), and would lift the degeneracy between H and A. Then one can avoid the strong bound from the direct detection cross section from the SM Z exchange in $HN \to AN$.

This scenario is a generalization of the well-known Inert Doublet Model, where the discrete symmetry Z_2 of IDMwZ_2 is replaced by local $U(1)_H$ gauge symmetry that is spontaneously broken into its Z_2 subgroup by nonzero VEV of Φ. Like the usual IDMwZ_2, the new model we presented in this paper has many interesting features, such as the co-annihilation of the scalars and new channels for the DM pair annihilations into $Z_H Z_H$, etc.

In the ordinary IDMwZ_2, there are two interesting CDM mass regions: $m_H \simeq 60\,\text{GeV}$ and $m_H \gtrsim 500\,\text{GeV}$. In these regions, the correct DM relic density can be achieved without any conflict with the experimental results including the bound from the direct and indirect dark matter detections. Especially, the recent results from the indirect detection experiments may give strong bounds on the DM mass and its interactions. We investigated the allowed region for the recent FERMI-LAT data in section 4.2. As we see in figure 6, the FERMI-LAT data strongly constrains the DM annihilation cross section, so that the allowed regions are reduced in both of the light and heavy scenarios. In fact, we found

JHEP11(2014)054

that $50 - 60\,\mathrm{GeV}$ CDM scenario is only allowed in the light CDM case, because of the low annihilation cross section at the present universe temperature.

In case of the IDMwU(1)$_H$, the nonzero U(1)$_H$ charge is assign to one Higgs doublet and one SM singlet, and U(1)$_H$ is spontaneously broken by the singlet. The U(1)$_H$ breaks down to discrete symmetry, so that we could interpret the continuous symmetry as the origin of the Z_2 Higgs symmetry in the IDMwZ_2. The additional massive gauge boson (Z_H) interacts with the extra Higgs doublet and weakly interacts with the SM particles through the mass and kinetic mixing with the SM gauge bosons in the IDMwU(1)$_H$. If we assume the kinetic mixing between U(1)$_H$ and U(1)$_Y$ is negligibly small before the EW and U(1)$_H$ symmetry breaking, we could expect that the Z_H interaction could be sizable as we see in figure 2. In the dark matter physics, the Z_H contribution might be dominant, and it may make the IDMwU(1)$_H$ distinguishable from the IDMwZ_2. In fact, we could find many allowed points for the bounds from the collider and dark matter experiments below $m_H = 60\mathrm{GeV}$ in the IDMwU(1)$_H$, where the IDMwZ_2 is totally excluded. We also investigated the consistency with the recent FERMI-LAT data, and we concluded that many points are still allowed in the light and heavy CDM mass regions. In particular a new possibility opens up that the inert 2HDM can accommodate the γ-ray excess from the galactic center, if we promote the discrete Z_2 symmetry to local U(1)$_H$ symmetry. This case will be discussed in detail elsewhere [91].

Our light CDM scenario predicts the exotic SM-Higgs decays: $h \to Z_H Z_H$ and $Z_H Z$. Z_H could decay to the SM fermions like the Z boson, so that it may be possible to observe Z_H at LHC, as studied by the CMS collaboration [92]. Developing the analysis of the SM-Higgs branching ratio, we may be able to draw the stronger bound on the exotic SM-Higgs decay according to the global fitting [46–48].

Acknowledgments

We are grateful to Seungwon Baek, Wan-Il Park, and Yong Tang for useful discussions and comments. We thank Korea Institute for Advanced Study for providing computing resources (KIAS Center for Advanced Computation Abacus System) for this work. This work was supported in part by Basic Science Research Program through the National Research Foundation of Korea (NRF) funded by the Ministry of Education Science and Technology 2011-0022996 (CY), by NRF Research Grant 2012R1A2A1A01006053 (PK and CY), and by SRC program of NRF funded by MEST (20120001176) through Korea Neutrino Research Center at Seoul National University (PK). The work of YO is supported by Grant-in-Aid for Scientific research from the Ministry of Education, Science, Sports, and Culture (MEXT), Japan, No. 23104011.

JHEP11(2014)054

References

[1] ATLAS collaboration, *Observation of a new particle in the search for the standard model Higgs boson with the ATLAS detector at the LHC*, *Phys. Lett.* **B 716** (2012) 1 [arXiv:1207.7214] [INSPIRE].

[2] CMS collaboration, *Observation of a new boson at a mass of* 125 *GeV with the CMS experiment at the LHC*, *Phys. Lett.* **B 716** (2012) 30 [arXiv:1207.7235] [INSPIRE].

[3] ATLAS collaboration, *Evidence for the spin-*0 *nature of the Higgs boson using ATLAS data*, *Phys. Lett.* **B 726** (2013) 120 [arXiv:1307.1432] [INSPIRE].

[4] CMS collaboration, *Measurement of the properties of a Higgs boson in the four-lepton final state*, *Phys. Rev.* **D 89** (2014) 092007 [arXiv:1312.5353] [INSPIRE].

[5] B. Grinstein and P. Uttayarat, *Carving out parameter space in type-II two Higgs doublets model*, *JHEP* **06** (2013) 094 [*Erratum ibid.* **09** (2013) 110] [arXiv:1304.0028] [INSPIRE].

[6] E. Ma, *Verifiable radiative seesaw mechanism of neutrino mass and dark matter*, *Phys. Rev.* **D 73** (2006) 077301 [hep-ph/0601225] [INSPIRE].

[7] R. Barbieri, L.J. Hall and V.S. Rychkov, *Improved naturalness with a heavy Higgs: an alternative road to LHC physics*, *Phys. Rev.* **D 74** (2006) 015007 [hep-ph/0603188] [INSPIRE].

[8] M. Cirelli, N. Fornengo and A. Strumia, *Minimal dark matter*, *Nucl. Phys.* **B 753** (2006) 178 [hep-ph/0512090] [INSPIRE].

[9] L. Lopez Honorez, E. Nezri, J.F. Oliver and M.H.G. Tytgat, *The inert doublet model: an archetype for dark matter*, *JCAP* **02** (2007) 028 [hep-ph/0612275] [INSPIRE].

[10] P. Ko, Y. Omura and C. Yu, *A resolution of the flavor problem of two Higgs doublet models with an extra* $\mathrm{U}(1)_H$ *symmetry for Higgs flavor*, *Phys. Lett.* **B 717** (2012) 202 [arXiv:1204.4588] [INSPIRE].

[11] J. Shu and Y. Zhang, *Impact of a CP-violating Higgs sector: from LHC to baryogenesis*, *Phys. Rev. Lett.* **111** (2013) 091801 [arXiv:1304.0773] [INSPIRE].

[12] S. Kanemura, T. Matsui and H. Sugiyama, *Loop suppression of Dirac neutrino mass in the neutrinophilic two Higgs doublet model*, *Phys. Lett.* **B 727** (2013) 151 [arXiv:1305.4521] [INSPIRE].

[13] P. Ko, Y. Omura and C. Yu, *Top forward-backward asymmetry and the CDF* Wjj *excess in leptophobic* $\mathrm{U}(1)'$ *flavor models*, *Phys. Rev.* **D 85** (2012) 115010 [arXiv:1108.0350] [INSPIRE].

[14] P. Ko, Y. Omura and C. Yu, *Chiral* $\mathrm{U}(1)$ *flavor models and flavored Higgs doublets: the top FB asymmetry and the* Wjj, *JHEP* **01** (2012) 147 [arXiv:1108.4005] [INSPIRE].

[15] P. Ko, Y. Omura and C. Yu, *Top* A_{FB} *at the Tevatron vs. charge asymmetry at the LHC in chiral* $\mathrm{U}(1)$ *flavor models with flavored Higgs doublets*, *Eur. Phys. J.* **C 73** (2013) 2269 [arXiv:1205.0407] [INSPIRE].

[16] P. Ko, Y. Omura and C. Yu, $B \to D^{(*)}\tau\nu$ *and* $B \to \tau\nu$ *in chiral* $\mathrm{U}(1)'$ *models with flavored multi Higgs doublets*, *JHEP* **03** (2013) 151 [arXiv:1212.4607] [INSPIRE].

[17] P. Ko, Y. Omura and C. Yu, *Top FB asymmetry vs. (semi)leptonic B decays in multi-Higgs-doublet models*, arXiv:1304.4413 [INSPIRE].

JHEP11(2014)054

[18] P. Ko, Y. Omura and C. Yu, *Multi-Higgs doublet models with local* $\mathrm{U}(1)_H$ *gauge symmetry and neutrino physics therein*, arXiv:1401.3572 [INSPIRE].

[19] S.L. Glashow and S. Weinberg, *Natural conservation laws for neutral currents*, *Phys. Rev.* **D 15** (1977) 1958 [INSPIRE].

[20] Y. Kajiyama, H. Okada and K. Yagyu, *Electron/muon specific two Higgs doublet model*, *Nucl. Phys.* **B 887** (2014) 358 [arXiv:1309.6234] [INSPIRE].

[21] P. Ko, Y. Omura and C. Yu, *Higgs phenomenology in type-I 2HDM with* $\mathrm{U}(1)_H$ *Higgs gauge symmetry*, *JHEP* **01** (2014) 016 [arXiv:1309.7156] [INSPIRE].

[22] N.G. Deshpande and E. Ma, *Pattern of symmetry breaking with two Higgs doublets*, *Phys. Rev.* **D 18** (1978) 2574 [INSPIRE].

[23] M.S. Carena, A. Daleo, B.A. Dobrescu and T.M.P. Tait, Z' *gauge bosons at the Tevatron*, *Phys. Rev.* **D 70** (2004) 093009 [hep-ph/0408098] [INSPIRE].

[24] LEP, ALEPH, DELPHI, L3, OPAL, LEP Electroweak Working Group, SLD Electroweak Group and SLD Heavy Flavor Group collaborations, *A combination of preliminary electroweak measurements and constraints on the standard model*, hep-ex/0312023 [INSPIRE].

[25] ALEPH, DELPHI, L3, OPAL and LEP Electroweak Working Group collaborations, J. Alcaraz et al., *A combination of preliminary electroweak measurements and constraints on the standard model*, hep-ex/0612034 [INSPIRE].

[26] Particle Data Group collaboration, J. Beringer et al., *Review of particle physics (RPP)*, *Phys. Rev.* **D 86** (2012) 010001 [INSPIRE].

[27] E.J. Chun, J.-C. Park and S. Scopel, *Dark matter and a new gauge boson through kinetic mixing*, *JHEP* **02** (2011) 100 [arXiv:1011.3300] [INSPIRE].

[28] A. Hook, E. Izaguirre and J.G. Wacker, *Model independent bounds on kinetic mixing*, *Adv. High Energy Phys.* **2011** (2011) 859762 [arXiv:1006.0973] [INSPIRE].

[29] ATLAS collaboration, *Search for high-mass dilepton resonances in* $20\,\mathrm{fb}^{-1}$ *of pp collisions at* $\sqrt{s} = 8$ *TeV with the ATLAS experiment*, ATLAS-CONF-2013-017, CERN, Geneva Switzerland (2013).

[30] CMS collaboration, *Search for resonances in the dilepton mass distribution in pp collisions at* $\sqrt{s} = 8$ *TeV*, CMS-PAS-EXO-12-061, CERN, Geneva Switzerland (2012).

[31] E. Lundstrom, M. Gustafsson and J. Edsjo, *The inert doublet model and LEP II limits*, *Phys. Rev.* **D 79** (2009) 035013 [arXiv:0810.3924] [INSPIRE].

[32] Q.-H. Cao, E. Ma and G. Rajasekaran, *Observing the dark scalar doublet and its impact on the standard model Higgs boson at colliders*, *Phys. Rev.* **D 76** (2007) 095011 [arXiv:0708.2939] [INSPIRE].

[33] E. Dolle, X. Miao, S. Su and B. Thomas, *Dilepton signals in the inert doublet model*, *Phys. Rev.* **D 81** (2010) 035003 [arXiv:0909.3094] [INSPIRE].

[34] M. Gustafsson, S. Rydbeck, L. Lopez-Honorez and E. Lundstrom, *Status of the inert doublet model and the role of multileptons at the LHC*, *Phys. Rev.* **D 86** (2012) 075019 [arXiv:1206.6316] [INSPIRE].

JHEP11(2014)054

[35] A. Arhrib, Y.-L.S. Tsai, Q. Yuan and T.-C. Yuan, *An updated analysis of inert Higgs doublet model in light of the recent results from LUX, PLANCK, AMS-02 and LHC*, arXiv:1310.0358 [INSPIRE].

[36] A. Arhrib, R. Benbrik and N. Gaur, $H \to \gamma\gamma$ *in inert Higgs doublet model*, *Phys. Rev.* **D 85** (2012) 095021 [arXiv:1201.2644] [INSPIRE].

[37] B. Swiezewska and M. Krawczyk, *Diphoton rate in the inert doublet model with a* 125 *GeV Higgs boson*, *Phys. Rev.* **D 88** (2013) 035019 [arXiv:1212.4100] [INSPIRE].

[38] R. Enberg, J. Rathsman and G. Wouda, *Higgs properties in a softly broken inert doublet model*, *JHEP* **08** (2013) 079 [arXiv:1304.1714] [INSPIRE].

[39] ATLAS collaboration, *Measurements of the properties of the Higgs-like boson in the two photon decay channel with the ATLAS detector using* $25\,\text{fb}^{-1}$ *of proton-proton collision data*, ATLAS-CONF-2013-012, CERN, Geneva Switzerland (2013).

[40] ATLAS collaboration, *Measurements of the properties of the Higgs-like boson in the four lepton decay channel with the ATLAS detector using* $25\,\text{fb}^{-1}$ *of proton-proton collision data*, ATLAS-CONF-2013-013, CERN, Geneva Switzerland (2013).

[41] CMS collaboration, *Updated measurements of the Higgs boson at* 125 *GeV in the two photon decay channel*, CMS-PAS-HIG-13-001, CERN, Geneva Switzerland (2013).

[42] CMS collaboration, *Properties of the Higgs-like boson in the decay* $H \to ZZ \to 4\ell$ *in pp collisions at* $\sqrt{s} = 7$ *and* 8 *TeV*, CMS-PAS-HIG-13-002, CERN, Geneva Switzerland (2013).

[43] CMS collaboration, *Measurement of the properties of a Higgs boson in the four-lepton final state*, *Phys. Rev.* **D 89** (2014) 092007 [arXiv:1312.5353] [INSPIRE].

[44] CMS collaboration, *Search for an invisible Higgs boson*, CMS-PAS-HIG-13-013, CERN, Geneva Switzerland (2013).

[45] ATLAS collaboration, *Search for invisible decays of a Higgs boson produced in association with a Z boson in ATLAS*, *Phys. Rev. Lett.* **112** (2014) 201802 [arXiv:1402.3244] [INSPIRE].

[46] J.R. Espinosa, M. Muhlleitner, C. Grojean and M. Trott, *Probing for invisible Higgs decays with global fits*, *JHEP* **09** (2012) 126 [arXiv:1205.6790] [INSPIRE].

[47] G. Bélanger, B. Dumont, U. Ellwanger, J.F. Gunion and S. Kraml, *Global fit to Higgs signal strengths and couplings and implications for extended Higgs sectors*, *Phys. Rev.* **D 88** (2013) 075008 [arXiv:1306.2941] [INSPIRE].

[48] S. Choi, S. Jung and P. Ko, *Implications of LHC data on* 125 *GeV Higgs-like boson for the standard model and its various extensions*, *JHEP* **10** (2013) 225 [arXiv:1307.3948] [INSPIRE].

[49] D. Larson et al., *Seven-year Wilkinson Microwave Anisotropy Probe (WMAP) observations: power spectra and WMAP-derived parameters*, *Astrophys. J. Suppl.* **192** (2011) 16 [arXiv:1001.4635] [INSPIRE].

[50] R. Bernabei et al., *DAMA/LIBRA results and perspectives*, arXiv:1301.6243 [INSPIRE].

[51] C.E. Aalseth et al., *Search for an annual modulation in a P-type point contact germanium dark matter detector*, *Phys. Rev. Lett.* **107** (2011) 141301 [arXiv:1106.0650] [INSPIRE].

[52] G. Angloher et al., *Results from* 730 *kg days of the CRESST-II dark matter search*, *Eur. Phys. J.* **C 72** (2012) 1971 [arXiv:1109.0702] [INSPIRE].

JHEP11(2014)054

[53] XENON10 collaboration, J. Angle et al., *A search for light dark matter in XENON10 data*, *Phys. Rev. Lett.* **107** (2011) 051301 [*Erratum ibid.* **110** (2013) 249901] [arXiv:1104.3088] [INSPIRE].

[54] XENON100 collaboration, E. Aprile et al., *Dark matter results from 100 live days of XENON100 data*, *Phys. Rev. Lett.* **107** (2011) 131302 [arXiv:1104.2549] [INSPIRE].

[55] CDMS collaboration, R. Agnese et al., *Silicon detector dark matter results from the final exposure of CDMS II*, *Phys. Rev. Lett.* **111** (2013) 251301 [arXiv:1304.4279] [INSPIRE].

[56] LUX collaboration, D.S. Akerib et al., *First results from the LUX dark matter experiment at the Sanford Underground Research Facility*, *Phys. Rev. Lett.* **112** (2014) 091303 [arXiv:1310.8214] [INSPIRE].

[57] G. Bélanger, A. Goudelis, J.-C. Park and A. Pukhov, *Isospin-violating dark matter from a double portal*, *JCAP* **02** (2014) 020 [arXiv:1311.0022] [INSPIRE].

[58] G. Bélanger, F. Boudjema, A. Pukhov and A. Semenov, *MicrOMEGAs$_3$: a program for calculating dark matter observables*, *Comput. Phys. Commun.* **185** (2014) 960 [arXiv:1305.0237] [INSPIRE].

[59] D. Majumdar and A. Ghosal, *Dark matter candidate in a heavy Higgs model — direct detection rates*, *Mod. Phys. Lett.* **A 23** (2008) 2011 [hep-ph/0607067] [INSPIRE].

[60] T. Hambye, F.-S. Ling, L. Lopez Honorez and J. Rocher, *Scalar multiplet dark matter*, *JHEP* **07** (2009) 090 [*Erratum ibid.* **05** (2010) 066] [arXiv:0903.4010] [INSPIRE].

[61] P. Agrawal, E.M. Dolle and C.A. Krenke, *Signals of inert doublet dark matter in neutrino telescopes*, *Phys. Rev.* **D 79** (2009) 015015 [arXiv:0811.1798] [INSPIRE].

[62] S. Andreas, M.H.G. Tytgat and Q. Swillens, *Neutrinos from inert doublet dark matter*, *JCAP* **04** (2009) 004 [arXiv:0901.1750] [INSPIRE].

[63] E. Nezri, M.H.G. Tytgat and G. Vertongen, e^+ *and* $\bar{p}$ *from inert doublet model dark matter*, *JCAP* **04** (2009) 014 [arXiv:0901.2556] [INSPIRE].

[64] C. Arina, F.-S. Ling and M.H.G. Tytgat, *IDM and iDM or the inert doublet model and inelastic dark matter*, *JCAP* **10** (2009) 018 [arXiv:0907.0430] [INSPIRE].

[65] L. Lopez Honorez and C.E. Yaguna, *The inert doublet model of dark matter revisited*, *JHEP* **09** (2010) 046 [arXiv:1003.3125] [INSPIRE].

[66] M. Klasen, C.E. Yaguna and J.D. Ruiz-Alvarez, *Electroweak corrections to the direct detection cross section of inert Higgs dark matter*, *Phys. Rev.* **D 87** (2013) 075025 [arXiv:1302.1657] [INSPIRE].

[67] L. Lopez Honorez and C.E. Yaguna, *A new viable region of the inert doublet model*, *JCAP* **01** (2011) 002 [arXiv:1011.1411] [INSPIRE].

[68] A. Goudelis, B. Herrmann and O. Stål, *Dark matter in the inert doublet model after the discovery of a Higgs-like boson at the LHC*, *JHEP* **09** (2013) 106 [arXiv:1303.3010] [INSPIRE].

[69] C. Garcia-Cely and A. Ibarra, *Novel gamma-ray spectral features in the inert doublet model*, *JCAP* **09** (2013) 025 [arXiv:1306.4681] [INSPIRE].

[70] T. Bringmann, X. Huang, A. Ibarra, S. Vogl and C. Weniger, *Fermi-LAT search for internal bremsstrahlung signatures from dark matter annihilation*, *JCAP* **07** (2012) 054 [arXiv:1203.1312] [INSPIRE].

JHEP11(2014)054

[71] C. Weniger, *A tentative gamma-ray line from dark matter annihilation at the Fermi Large Area Telescope*, *JCAP* **08** (2012) 007 [arXiv:1204.2797] [INSPIRE].

[72] E. Tempel, A. Hektor and M. Raidal, *Fermi* 130 *GeV gamma-ray excess and dark matter annihilation in sub-haloes and in the galactic centre*, *JCAP* **09** (2012) 032 [*Addendum ibid.* **11** (2012) A01] [arXiv:1205.1045] [INSPIRE].

[73] M. Su and D.P. Finkbeiner, *Strong evidence for gamma-ray line emission from the inner galaxy*, arXiv:1206.1616 [INSPIRE].

[74] D.P. Finkbeiner, M. Su and C. Weniger, *Is the* 130 *GeV line real? A search for systematics in the Fermi-LAT data*, *JCAP* **01** (2013) 029 [arXiv:1209.4562] [INSPIRE].

[75] FERMI-LAT collaboration, M. Ackermann et al., *Search for gamma-ray spectral lines with the Fermi Large Area Telescope and dark matter implications*, *Phys. Rev.* **D 88** (2013) 082002 [arXiv:1305.5597] [INSPIRE].

[76] PAMELA collaboration, O. Adriani et al., *An anomalous positron abundance in cosmic rays with energies* 1.5-100 *GeV*, *Nature* **458** (2009) 607 [arXiv:0810.4995] [INSPIRE].

[77] FERMI-LAT collaboration, A.A. Abdo et al., *Measurement of the cosmic ray* e^+ *plus* e^- *spectrum from* 20 *GeV to* 1 *TeV with the Fermi Large Area Telescope*, *Phys. Rev. Lett.* **102** (2009) 181101 [arXiv:0905.0025] [INSPIRE].

[78] AMS collaboration, M. Aguilar et al., *First result from the alpha magnetic spectrometer on the International Space Station: precision measurement of the positron fraction in primary cosmic rays of* 0.5–350 *GeV*, *Phys. Rev. Lett.* **110** (2013) 141102 [INSPIRE].

[79] D. Hooper, P. Blasi and P.D. Serpico, *Pulsars as the sources of high energy cosmic ray positrons*, *JCAP* **01** (2009) 025 [arXiv:0810.1527] [INSPIRE].

[80] S. Profumo, *Dissecting cosmic-ray electron-positron data with Occam's razor: the role of known pulsars*, *Central Eur. J. Phys.* **10** (2011) 1 [arXiv:0812.4457] [INSPIRE].

[81] FERMI-LAT collaboration, M. Ackermann et al., *Constraining dark matter models from a combined analysis of milky way satellites with the Fermi Large Area Telescope*, *Phys. Rev. Lett.* **107** (2011) 241302 [arXiv:1108.3546] [INSPIRE].

[82] A. Geringer-Sameth and S.M. Koushiappas, *Exclusion of canonical WIMPs by the joint analysis of milky way dwarfs with Fermi*, *Phys. Rev. Lett.* **107** (2011) 241303 [arXiv:1108.2914] [INSPIRE].

[83] Y.-L.S. Tsai, Q. Yuan and X. Huang, *A generic method to constrain the dark matter model parameters from Fermi observations of dwarf spheroids*, *JCAP* **03** (2013) 018 [arXiv:1212.3990] [INSPIRE].

[84] FERMI-LAT collaboration, M. Ackermann et al., *Dark matter constraints from observations of* 25 *milky way satellite galaxies with the Fermi Large Area Telescope*, *Phys. Rev.* **D 89** (2014) 042001 [arXiv:1310.0828] [INSPIRE].

[85] X. Huang, Q. Yuan, P.-F. Yin, X.-J. Bi and X. Chen, *Constraints on the dark matter annihilation scenario of Fermi* 130 *GeV* γ*-ray line emission by continuous gamma-rays, milky way halo, galaxy clusters and dwarf galaxies observations*, *JCAP* **11** (2012) 048 [*Erratum ibid.* **05** (2013) E02] [arXiv:1208.0267] [INSPIRE].

[86] J.F. Navarro, C.S. Frenk and S.D.M. White, *A universal density profile from hierarchical clustering*, *Astrophys. J.* **490** (1997) 493 [astro-ph/9611107] [INSPIRE].

JHEP11(2014)054

[87] J.D. Simon and M. Geha, *The kinematics of the ultra-faint milky way satellites: solving the missing satellite problem*, *Astrophys. J.* **670** (2007) 313 [arXiv:0706.0516] [INSPIRE].

[88] M.G. Walker et al., *A universal mass profile for dwarf spheroidal galaxies*, *Astrophys. J.* **704** (2009) 1274 [*Erratum ibid.* **710** (2010) 886] [arXiv:0906.0341] [INSPIRE].

[89] J.D. Simon et al., *A complete spectroscopic survey of the milky way satellite Segue 1: the darkest galaxy*, *Astrophys. J.* **733** (2011) 46 [arXiv:1007.4198] [INSPIRE].

[90] S.E. Koposov et al., *Accurate stellar kinematics at faint magnitudes: application to the Bootes I dwarf spheroidal galaxy*, *Astrophys. J.* **736** (2011) 146 [arXiv:1105.4102] [INSPIRE].

[91] P. Ko, Y. Omura and C. Yu, work in progress.

[92] CMS collaboration, *Search for a non-standard-model Higgs boson decaying to a pair of new light bosons in four-muon final states*, CMS-PAS-HIG-13-010, CERN, Geneva Switzerland (2013).

JHEP11(2014)054